Journal of Nanostructure in Chemistry (2024) 14:1–19
https://doi.org/10.1007/s40097-022-00493-2

REVIEW

Nanoscale metal–organic frameworks as smart nanocarriers for cancer therapy

Yang Liu[1] · Pengfei Lei[4] · Xuewei Liao[2] · Chen Wang[3]

Received: 15 December 2021 / Accepted: 15 April 2022 / Published online: 1 June 2022

Abstract

Cancer is one of the serious diseases to human life. Early and precise cancer diagnosis and timely therapy are in urgent need nowadays. Due to the advantages of porous structures and tunable properties, metal–organic frameworks (MOFs) are becoming type of rapidly developing and attractive supports used in biomedicine, which have been widely applied in the fields of chemistry, biology, materials science, etc. Particularly, nanoscale MOFs (nMOFs) with more accessible active sites and improved stability are ideal platforms for biological and clinical applications in vitro and in vivo. This review article summarizes the recent progresses in nMOFs based nanoplatforms for drug delivery and cancer therapy. Different techniques using nMOFs are systematically summarized including chemotherapy, photodynamic therapy (PDT), photothermal therapy (PTT), chemodynamic therapy (CDT), radiotherapy (RT), and the combined therapy methods. Finally, a brief conclusion and outlook for biomedical applications of this special field is provided. We expect this review could be helpful for future designing and fabrication of multi-functional nMOFs platforms for drug delivery, disease therapy, and other biomedical applications.

Keywords Nanoscale metal–organic frameworks (nMOFs) · Nanocarrier · Drug delivery · Cancer therapy · Biomedicine

Introduction

Cancer is one of the serious diseases to human life, causing millions of deaths annually [1]. Patient survival will be substantially improved by an early and precise cancer diagnosis and timely therapy [2]. Traditional cancer therapies have great side effects on patients, and even produce serious traumas. Many researchers have developed minimally invasive or non-invasive treatments with fewer side effects and effectiveness to relieve the pain in therapeutic processes, such as intelligent chemotherapy, photodynamic therapy (PDT), photothermal therapy (PTT), chemodynamic therapy (CDT), radiotherapy (RT), and the combined therapy [3–9]. During the last few decades, numerous nanomaterials including metal nanoparticles, inorganic mesoporous silica, organic micelles and quantum dots have been developed for biosensing, drugs delivery, and tumor therapy [10–19]. However, low loading capacities, undesirable toxicity and unacceptable degradability of the materials have limited their real applications in bioanalysis and disease therapy [20–22].

Due to the advantages of porous structures and tunable properties, metal–organic frameworks (MOFs) have been widely applied in the fields of chemistry, biology, materials science, etc., and are becoming a type of rapidly developing and attractive supports used in biomedicine [23, 24]. Particularly, nanoscale MOFs (nMOFs) with more accessible active sites and improved stability stand out in drug delivery and tumor therapy owing to the following advantages [25]. Compared to other nanoparticles, nMOFs can be facilely designed to possess various functions for synergistic applications. First, the variety of metal ions and ligands of nMOFs endows the materials with various functions and can be used for special biosensors, imaging agents or therapeutic agents in biological and clinical applications. Second,

✉ Xuewei Liao
liaoxuewei@njnu.edu.cn

1 School of Environment, Nanjing Normal University, Nanjing 210023, China

2 Analytical and Testing Center, Nanjing Normal University, Nanjing 210023, China

3 College of Chemistry and Materials Science, Nanjing Normal University, Nanjing 210023, China

4 Department of Orthopedic Surgery, The First Affiliated Hospital, College of Medicine, Zhejiang University, Hangzhou, China

the highly ordered pores and large specific surface area of nMOFs can improve the loading rate of cargoes, such as anti-cancer drugs or functional agents. Third, target molecules can be modified on the surface of nMOFs via chemical bonds to enhance the tumor-targeting efficiency. They can be passively targeted to the tumor site in vivo because of the size-dependent enhanced permeability and retention effect. Moreover, selecting biocompatible molecules as parts of nMOFs can ensure the biosafety from the source [26]. The stable but degradable structures of nMOFs can guarantee the excreting from body. The acceptable biocompatibility and biodegradability of nMOFs provide possibilities for the biomedical applications in vivo.

In this review article, we summarized the recent advances of nMOFs-based composite materials applying for cancer therapy (Fig. 1). Various tumor therapeutic strategies were highlighted including intelligent chemotherapy, PDT, PTT, CDT, and the combined therapy. At last, the prospects and key challenges in this area was discussed. We expect that this review can inspire more exciting explorations in the biomedical community for applying nMOFs for tumor therapy and disease diagnosis.

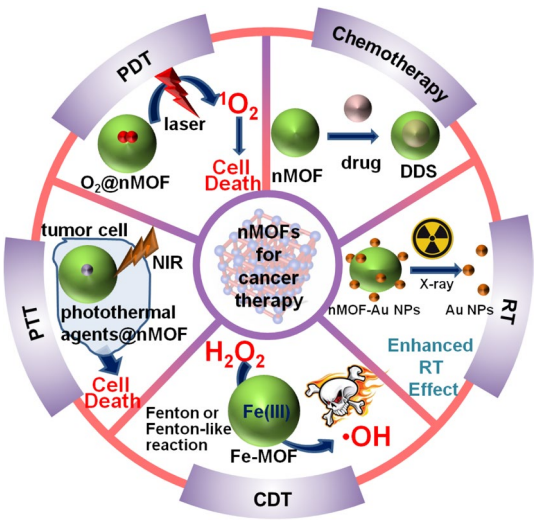

Fig. 1 Schematic illustration of the strategies based on nanoscale metal–organic frameworks (nMOFs) nanocarriers for cancer therapy. Summarization of the various tumor therapeutic strategies including intelligent chemotherapy, photodynamic therapy (PDT), photothermal therapy (PTT), chemodynamic therapy (CDT), radiotherapy (RT), and the combined therapy methods based on multifunctional biomedical nanoscale metal–organic frameworks (nMOFs) platforms are presented

General NMOFs synthesis and fabrication strategies for therapy

With the development of MOFs materials, controlled synthetic strategy is designed for biological and clinical applications to improve their capability, biocompatibility, bioactivity and targeting ability in vitro and in vivo. As porous nanomaterials with structurally well-defined pore networks, MOFs can be designed with an extended array of inorganic and organic components. For disease therapy, toxicological concerns are the first considerations of the MOFs synthesis and fabrication strategies. As extensive evidences demonstrating that particle size does matter concerning particle toxicity and biodistribution [27], controlled particle size within nanoscale is on the list of priorities in the synthesis of therapeutic MOFs materials. Generally, the nMOFs synthetic techniques such as nano-precipitation method (based on the poor solubility in the organic dissolvent of the coordination nanoparticles to obtain nMOFs comparing to the metal salts and organic ligands [28]), microwave-ultrasound-assisted solvothermal method (based on the microwave-ultrasound-assisted self-assembly of coordination reaction to obtain nMOFs under certain temperature and pressure [29]), micro-emulsion method (based on the anti-sedimentation effect of the dispersed nanoparticles in the micro-emulsion to obtain nMOFs [30]), etc., are mainly in use (Fig. 2). Then, for disease therapy, the relevant agents are encapsulated into the nMOFs materials for the controlled release of such agents via different therapeutic mechanisms. Through optimizing the reaction parameters such as temperature, pressure, solvent, pH, reaction time, reactant concentration, etc., the nMOFs with definite composition, properties and morphology can be obtained [31–33]. Significantly, for biological applications the fabrication of nMOFs from toxic metals (such as Co, Ni, Cd, etc.) should be ruled out regarding the toxicological concerns. Generally, non-toxic or poorly-toxic units (including biocompatible and bioactive cations and ligands) give priority to the design of nMOFs. For example, endogenous cations (such as Fe, Zn, Mn, etc. salts, essential for life [34]) or exogenous elements (such as Au NPs, Pt NPs, etc., for therapeutic purposes [35]), and active ingredients (AIs) as ligands (such as saccharides, peptides, amino acids, proteins, nucleobases, porphyrins, organic drugs, etc. [36, 37]) are always used in the rational nMOFs fabrication. So far, large amounts of works on the synthesis and fabrication of nMOFs for disease therapy have been done [38], there still remains many challenges regarding to their bio-ability and bio-safety [39, 40].

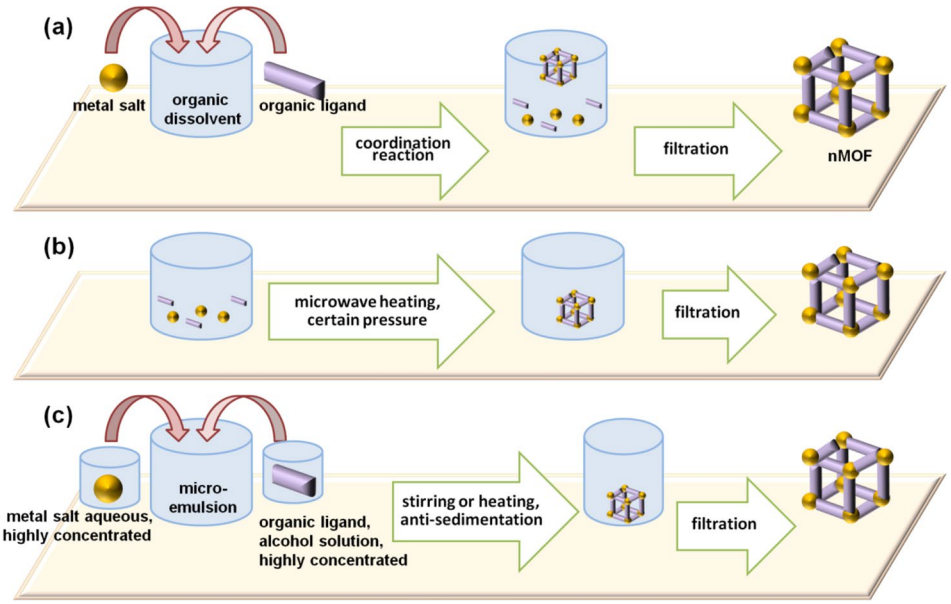

Fig. 2 Schematic illustration of the nMOFs synthetic techniques: **a** nano-precipitation method, **b** microwave-ultrasound-assisted solvothermal method, and **c** micro-emulsion method

Chemotherapy

At present, chemotherapy is still one of the most efficient methods for cancer therapy [41]. A variety of effective chemotherapy drugs have been widely used in clinical treatments for solid and non-solid tumors including doxorubicin hydrochloride (DOX) [42], fluorouracil (5-FU) [43], cisplatin [44] and methotrexate [45], etc. However, directly using anticancer drugs has serious side effects, poor pharmacokinetics and disordered biodistribution that heavily hampered the efficient therapeutic effect [46]. Currently, drug delivery systems (DDS) composed of various nanocarriers have been developed to avoid adverse reactions and improve the therapeutic effect in tumor areas, including micelles [47], polymers [48], carbon nanomaterials [49], inorganic nanoparticles [50], etc.

As the promising encapsulating carriers for drug molecules, nMOFs have many desirable characteristics such as extremely high surface area, adjustable drug-loading pore size, high loading capacity and extensive interactions (by Van der Waals force, electrostatic force, hydrogen bonding, π–π stacking, or coordination bond), which can be used for drug adsorption [51–53]. By choosing biocompatible metals and organic ligands, the bioavailability and efficiency of drugs can be greatly improved, and the toxicity could also be neatly avoided [54]. To optimize the release effect, Jimenez's group made a lot of efforts. They encapsulated calcein in the UiO-66, a Zr-based MOF, and then amorphized UiO-66 by ball-milling [55]. Compared with crystalline UiO-66, it was found that the amorphization MOF can control the release of calcein over more than 15 times longer (up to 30 days). Besides, after mild temperature treatment, part of the pores of NU-1000 and NU901 (NU-1000 and NU-901 are two MOFs formed by a parent-framework node of octahedral Zr_6-cluster capped by eight μ_3-OH ligands, where 8 of the 12 edges are linked to ligands) collapsed, which increased loading rate (up to 81 wt %) and delayed the release of calcein and α-cyano-4-hydroxycinnamic acid (α-CHC) (Fig. 3a) [56]. In addition, the special microenvironment of tumor cells can be used to design nMOFs-based intelligent DDS with multiple functions, which would enhance the selectivity of chemotherapeutic drugs. Up to now, respective factors including pH, redox, molecular/ion, light, pressure, or integration of these, are developed as intelligent DDS for efficient chemotherapy.

For pH-responsive DDS, it is designed from the weak acidity of the tumor microenvironment. Unstable nMOFs in weak acid solution, such as ZIF-n (ZIF: zeolitic imidazolate frameworks) and MIL-n (MIL: materials of Institute Lavoisier) series, are commonly used as pH-responsive controlled release switches [57]. A core–shell intelligent DDS containing bovine serum albumin (BSA)/DOX nanoparticles as core and ZIF-8 as shell was prepared [58]. ZIF-8 served as a safe storage capsule for DOX and under acidic conditions, the skeleton decomposed and released BSA/DOX. Compared to free DOX, the BSA/DOX@ZIF showed a much higher efficacy against the breast cancer cell line MCF-7. Modifying pH-sensitive materials outside the nMOFs is another strategy to control the drug release. Du's group designed a unique nanocomposite with excellent solubility and biocompatibility (Fig. 3b) [59]. pH-responsive poly(ethylene glycol) methacrylate(PEGMA) modified onto the surface of nanocomposite enhanced the selective DOX release performance at the weakly acidic environment in vitro (39.3% of cargo in 10 h and 98.0% in 5 days). The hydrophobic interaction

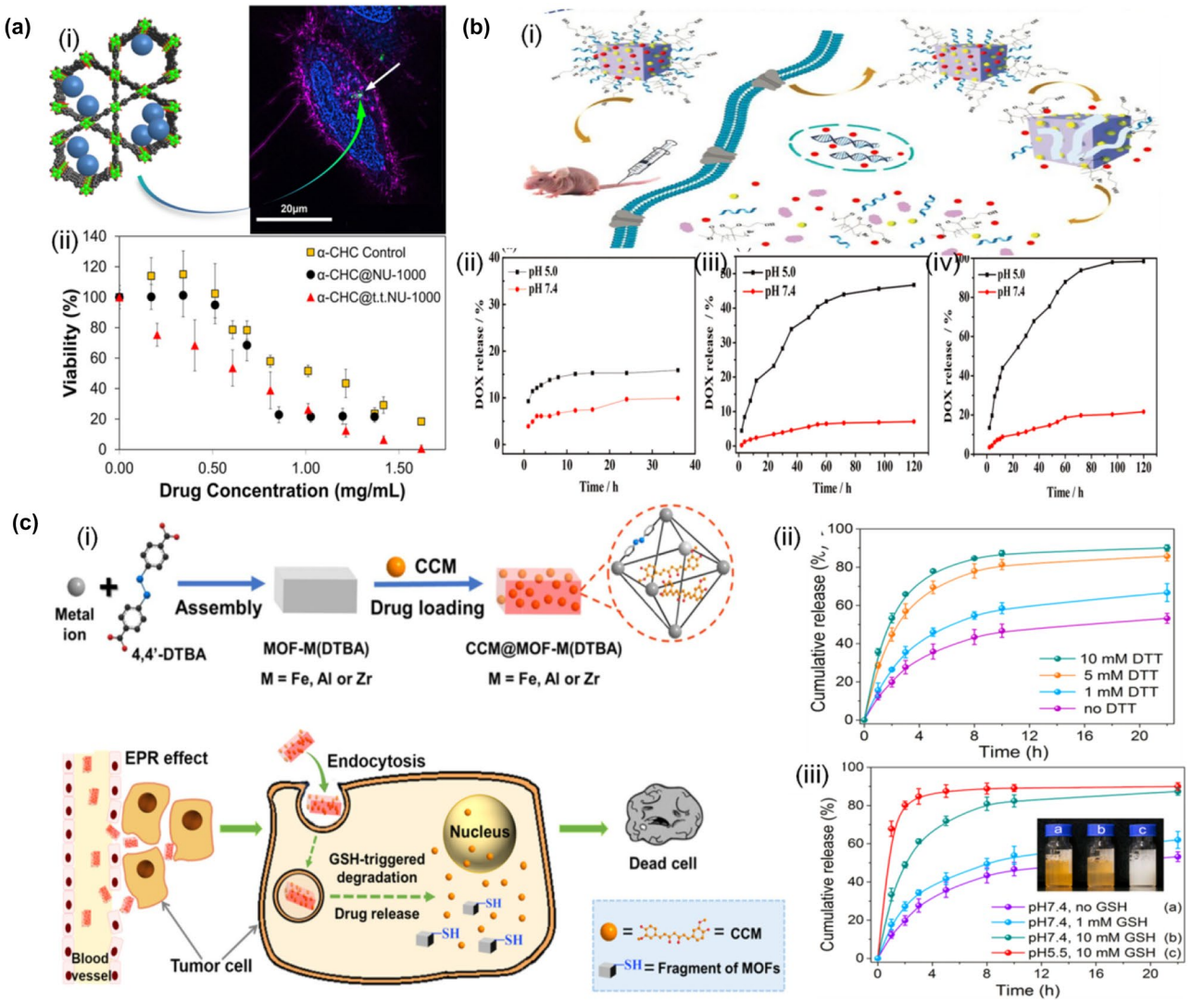

Fig. 3 Schematic illustration of the nMOFs as the common pH-responsive and redox-responsive drug delivery systems (DDS) for chemotherapy. **a** (i) Structured illumination microscopy (SIM) 3-color image of HeLa cells demonstrating NU-1000 (NU-1000: a MOF formed by a parent-framework node of octahedral Zr_6-cluster capped by eight μ_3-OH ligands, where 8 of the 12 edges are linked to TBAPy ligands; *TBAPy* 1,3,6,8-*tetra*(4-carboxy phenyl) pyrene) uptake into the cellular boundary. Nucleus colored in blue, lysosomes colored in magenta, NU-1000 colored in green. (ii) Non-radioactive cell proliferation assays measuring enzymatic metabolic activity for α-CHC-loaded NU-1000 (*α-CHC* α-cyano-4-hydroxycinnamic acid) in both crystalline and temperature treated complexes for 48 h of in vitro incubation. The free drug, α-CHC Control, is shown incubated for both time points in yellow. Reproduced with permission [56]. Copyright 2017, American Chemical Society. **b** (i) PEGMA@graphene quantum dots@γ-CD-MOF-based DOX loading (*PEGMA* pH-responsive poly(ethylene glycol) methacrylate, *CD* cyclodextrin, *DOX* doxorubicin) and pH-responsive controlled release system. The pH dependent DOX release of (ii) DOX/γ-CD-MOF, (iii) DOX/graphene quantum dots@γ-CD-MOF, and (iv) DOX/AS1411@PEGMA@GQDs@γ-CD-MOF (*AS1411* an aptamer recognizing the nucleolin receptor sites on the cancer cell membrane; *PEGMA* poly(ethylene glycol) dimethacrylate). Reproduced with permission [59]. Copyright 2019, Royal Society of Chemistry. **c** (i) Schematic illustration of the preparation and the redox-responsive degradation of CCM@MOF-M(DTBA) in tumor cells for cancer therapy (*CCM* curcumin, *M* represent Fe, Al, or Zn, *DTBA* dithiobisbenzoic acid). Drug release from CCM@MOF-Zr(DTBA) in phosphate-buffered saline (PBS, pH 7.4) containing different concentrations of (ii) dithiothreitol (DTT) or (iii) glutathione (GSH). Reproduced with permission [34]. Copyright 2018, American Chemical Society

between PEGMA and DOX led to a high loading efficiency (up to 89.1%). In addition, Willner's group reported a pH triggered DNA functionalized nMOFs to control the release performance [60].

For a redox-responsive system, glutathione (GSH) is a typical and strong reducing agent that mainly controlling the redox-responsive release process by cleaving disulfide bonds and reducing oxidizing substances [61–63]. Compared with normal tissues, overexpressed GSH (ranging from 2 to

10 mM in the cytoplasm) is 100–1000 times higher than blood and extracellular matrix (2 μM), which is one of the main characteristics of tumor tissues [61]. A redox-responsive nMOFs-based carrier was successfully constructed by selecting 4,4′-dithiobisbenzoic acid (4,4′-DTBA) containing disulfide bonds as the organic ligand (Fig. 3c) [34]. MOF-M(DTBA) (M represents Fe, Al, or Zr) encapsulating anticarcinogen curcumin could be easily absorbed by tumor cells owing to the enhanced permeability and retention effect and cellular endocytosis. Overexpressed GSH cleaved the disulfide bonds in 4,4′-DTBA and triggered the collapse of MOF skeletons to release free curcumin. This GSH-responsive nanocomposite overcame the low solubility and poor stability of free curcumin. In addition to GSH, responsive drug release can also be realized through redox reaction between the enzyme and the substrate [64, 65] and ATP coordination [66]. Willner's group encapsulated DOX in the nMOFs and then locked with the hydrogel coating including anti-ATP aptamer [67]. In the presence of ATP that is overexpressed in cancer cells, the resulting caged configuration was degraded via the formation of the ATP-aptamer complex, resulting in the successful release of DOX.

Except for the common pH-responsive and redox-responsive drug release systems, other endogenous substances such as ions [60], H_2S [68] and exogenous stimulations including thermal [69], light [70], and external pressure stimulation [71] have been used to design intelligent DDS as well. For instance, it was reported that Zr-based MOF named ZJU-801 could be served as an eminent drug delivery system (Fig. 4a) [72]. The introduction of naphthalene moiety into ligand weakened the side effects to normal tissues, protecting diclofenac sodium from premature release through strengthening the interaction between MOF and diclofenac sodium. The as-prepared DDS did not need complex post-modifications and could easily realize thermal stimuli-triggered drug release. At 25 and 37 °C, a premature release could be

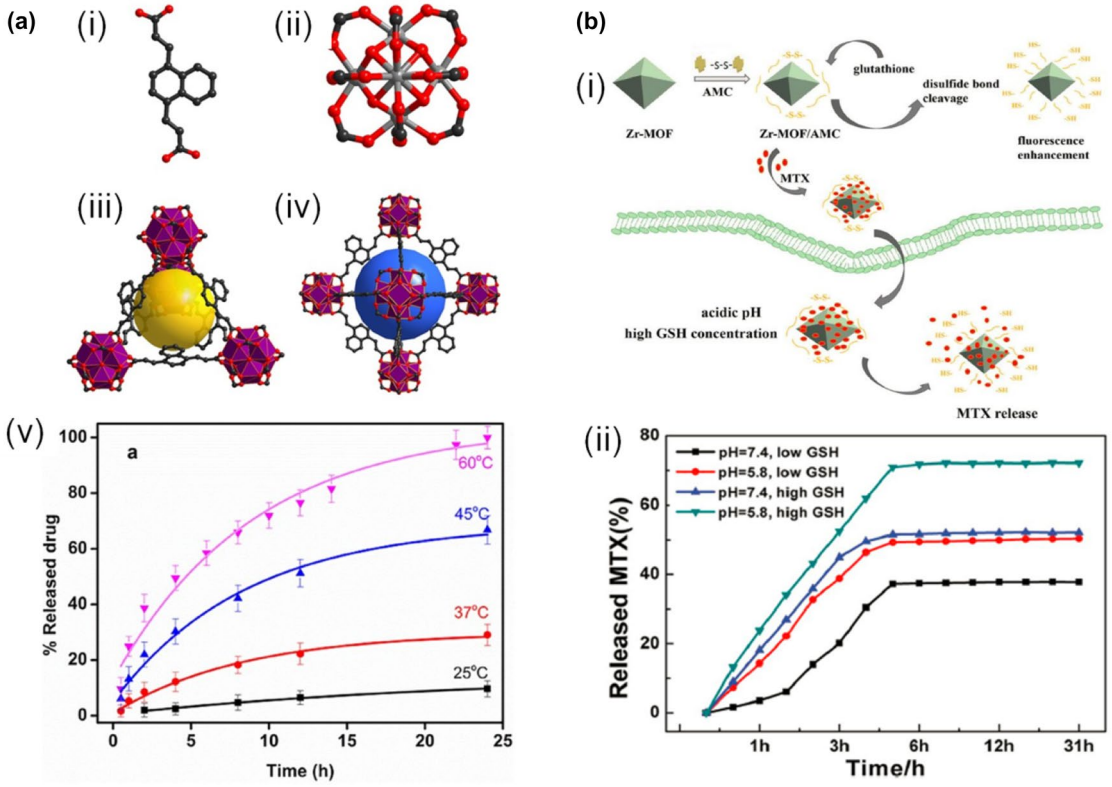

Fig. 4 Schematic illustration of the nMOFs as other endogenous and exogenous stimulation-activated drug delivery systems (DDS) for chemotherapy. **a** Construction of the framework of ZJU-801 (a Zr-based MOF). (i) two-coordination ligand (2E,2′E)-3,3′-(naphthalene-1,4-diyl)diacrylic acid (H_2NPDA) for ZJU-801. (ii) twelve-coordination secondary building units (SBUs) $Zr_6O_4(OH)_4(CO_2)_{12}$ of the framework. (iii) smaller tetrahedral cage with a diameter of about 10.0 Å constructed from four SBUs and six ligands. (iv) larger octahedral cage with a diameter of about 13.6 Å composed of six SBUs and twelve ligands. (v) Diclofenac sodium released from ZJU-801 in phosphate-buffered saline (PBS; pH 7.4) at 25, 37, 45, and 60 °C. Reproduced with permission [72]. Copyright 2017, John Wiley & Sons. **b** (i) Schematic illustration of the synthetic procedure of Zr-MOF/AMC/methotrexate (*AMC* acetaldehyde-modified cystine) and the proposed mechanisms by which Zr-MOF/AMC nanoparticles act as a glutathione probe and dual-responsive drug carrier. (ii) Methotrexate release profiles from Zr-MOF/AMC at different pH values and different concentrations of glutathione. Reproduced with permission [74]. Copyright 2020, Royal Society of Chemistry

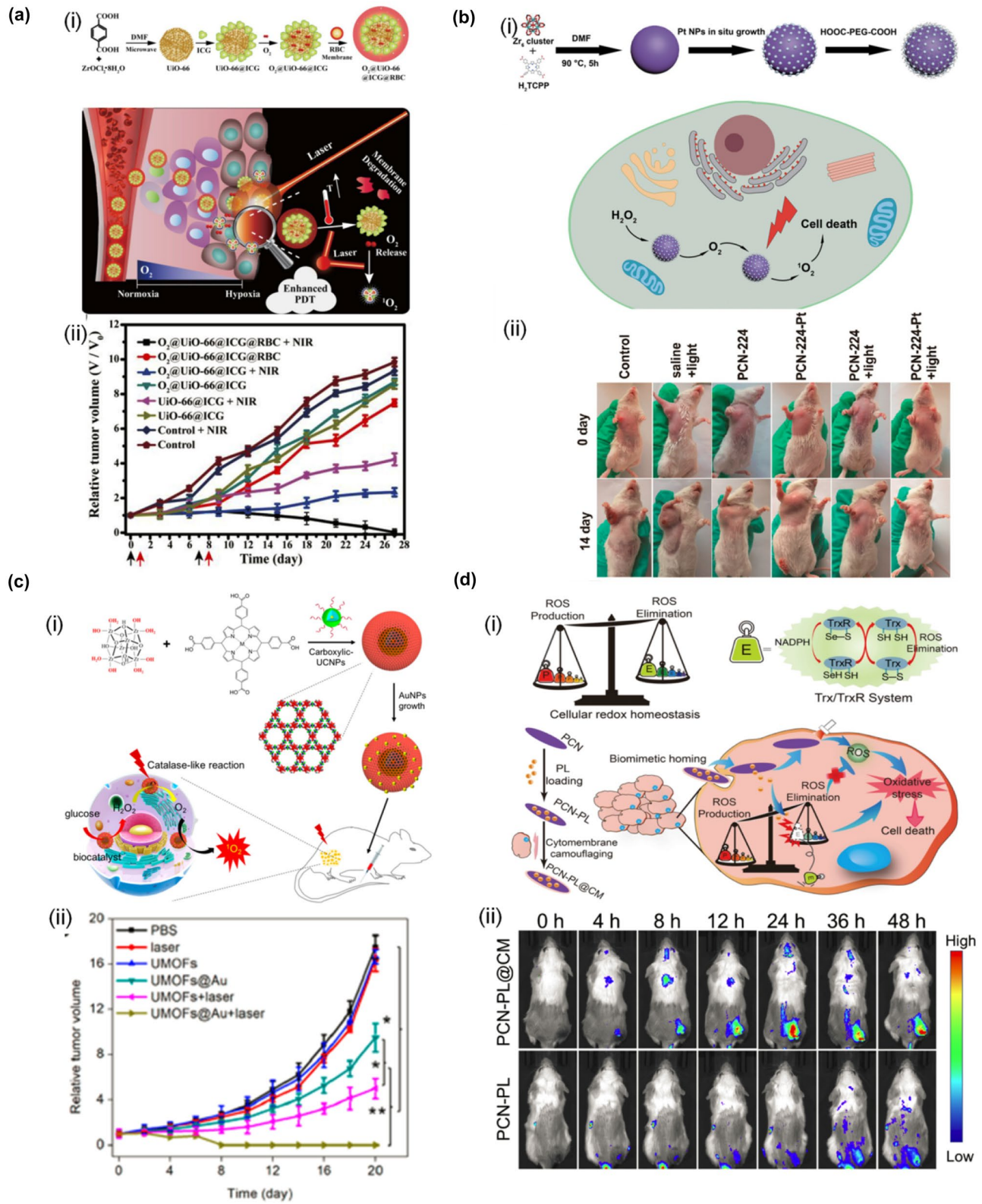

ignored because ZJU-801 maintained its initial structure. While at 45 and 60 °C, partial collapsing of ZJU-801 significantly accelerated drug release. Besides, a first-of-its kind nMOF DDS for photo-controlled therapeutics was reported by Grove's group [73]. The photo-responsive azobenzene dicarboxylate acted as a linker in UiO-type MOF. The

◂**Fig. 5** Schematic illustration of the nMOFs as photosensitizers for photodynamic therapy (PDT). **a** (i) Schematic illustration of the preparation of O_2@UiO-66@ indocyanine green@RBC (red blood cell) and the mechanism of NIR-triggered O_2 releasing and enhanced PDT (NIR: near infrared; PDT: photodynamic therapy). (ii) In vivo antitumor study of relative tumor volume of MCF-7 tumor-bearing mice in different groups, while the black arrows were for intravenous injection and red arrows was for the laser irradiation. Reproduced with permission [90]. Copyright 2018, Elsevier B.V. **b** (i) Schematic illustration of the preparation process of PCN-224-Pt (a porphyrin MOF) and the use of PCN-224-Pt for enhanced PDT. (ii) Photographs of the Hepatoma 22 (H22) tumor-bearing mice before treatment and on day 14 after the various treatments. Reproduced with permission [92]. Copyright 2018, American Chemical Society. **c** (i) Scheme of core–shell UMOFs@Au NPs for synergistic cancer therapy through cascade catalytic reactions. (ii) Tumor growth curves of mice bearing U87MG tumors subjected to various treatments. Reproduced with permission [99]. Copyright 2020, American Chemical Society. **d** Schematic illustration of interfering with redox homeostasis in cancer cells for improved photodynamic therapy. (ii) In vivo time-dependent fluorescence images after intravenous injection with PCN-PL and PCN-PL@CM. Reproduced with permission [101]. Copyright 2019, Elsevier B.V

prepared UiO- azobenzene dicarboxylate was stable in dark and degraded upon irradiation to release 5-fluorouracil for chemotherapy.

To guarantee that the drugs work on cancer cells more accurately, it is feasible to develop dual stimulation-activated drug release systems. A dual-reactive drug releasing system of Zr-MOF/AMC hybrid was successfully constructed by coating acetaldehyde-modified cystine (AMC) on Zr-MOF surface through amide reaction (Fig. 4b) [74]. AMC had functional groups including disulfide bonds and nitrile groups. Disulfide bonds could be broken by GSH and nitrile groups be hydrolyzed by acid. The antitumor drug methotrexate loaded into porous Zr-MOF/AMC was then be released in cancer cells with high GSH concentration and low pH. In another example, pH and NIR light dual stimuli-responsive AuNR@ZIF-8 core–shell structure were fabricated [75]. Under the 808 nm laser irradiation and weak acid environment, breaking of coordination bonds between metal center and organic active sites led to anticancer drug releasing. Thus, high-performance cancer treatment was achieved both in vitro and in vivo.

Photodynamic therapy (PDT)

With the development of optical technology, PDT has become an emerging cancer therapy due to its advantages of minimally invasive and quick action [76–81], which is the synergistic action of photosensitizer, oxygen, and light are required for PDT. Under laser irradiation, energies transfer from the photosensitizer excited triplet state to surrounding molecular oxygen, leading to the generation of singlet oxygen ($^1O_2$) during the collisional processes [82]. Tumor cells can be destroyed by $^1O_2$ owing to their strong oxidizing ability to nucleic acids, enzymes and, cell membranes [81, 83]. Porphyrin derivatives are common photosensitizers but often results in imperfect outcomes when be used alone because of hydrophobic and easy-aggregated property [84, 85]. As the fourth generation of photosensitizers [82], nMOFs are potential nanomaterials for PDT to overcome the unsatisfying solubility and aggregation problems while minimizing quenching of excitation energy. Besides, periodic arrays of pores allow nMOFs to load more photosensitizers and accelerate the diffusion rate of singlet oxygen [86, 87].

The first porphyrin-based nMOFs (Hf-p-nMOF) was fabricated as a highly effective photosensitizer for PDT [86]. By incorporating a porphyrin derivative, 5,15-di (*p*-benzoato) porphyrin (H_2DBP), as bridging ligand into a robust and porous UiO nMOF. The coordination of Hf centers to the carboxylate groups of H_2DBP ligands promoted intersystem crossing and then the $^1O_2$ generation efficiency was increased. Although DBP-UiO was an effective PDT agent for head and neck cancer, the photophysical properties were not optimal due to the lowest-energy absorption at excitation light wavelength and the relatively small extinction coefficient. To solve these problems, Lin's group designed a chlorin-based nMOF, DBC-UiO, using 5,15-di (*p*-benzoato)-chlorin (H_2DBC) as organic ligands [87]. Compared to porphyrin-based nMOF, the reduction of DBP to DBC resulted in a 13 nm redshift and 11-fold increased extinction coefficient of the lowest energy Q band. Thus, DBC-UiO had increased $^1O_2$ production capacity while retaining the crystallinity, stability, expansion rate and, nanoplate morphology of DBP-UiO. In addition, benzoporphyrin derivatives were also expected to act as PDT agents due to the extension of π-conjugation, red-shifted absorption bands ($\lambda > 650$ nm), and higher chemical stability compared with porphyrins [88].

However, the rapid proliferation of cancer cells and the distortion of cancer blood vessels usually lead to the hypoxia of the tumor microenvironment, which will limit the PDT efficiency [89]. To change the hypoxic microenvironment, Zhang's group fabricated a nMOF-based biomimetic O_2-evolving PDT nanoplatform with long circulating properties (Fig. 5a) [90], in which UiO-66 was coupled with indocyanine green via coordination reaction and the porous structure was propitious to store O_2. Under 808 nm laser irradiation, $^1O_2$ was generated by indocyanine green. At the same time, the photothermal properties of indocyanine green promoted the burst release of O_2 from UiO-66, which significantly improved the PDT effect on hypoxic tumor. Besides, the decomposition of endogenous H_2O_2 into O_2 in tumor cells catalyzed by catalase was beneficial for PDT. In another work, by encapsulating the black phosphorus quantum dots and catalase into nMOFs, a quantum dots-MIL@cat-MIL (a quantum dots and catalase co-encapsulated

Materials of Institute Lavoisier (MIL-101)-type MOF heterostructure) nanoplatform was designed as tandem catalytic system. Qu's group uniformly modified catalase-like Pt nanoparticles on the surface of PCN-224 nanoparticles via in situ reduction (Fig. 5b) [92]. PCN-224 prevented the aggregation of adjacent Pt nanoparticles and then enhanced the catalase-like activity and stability of Pt nanozymes.

Enough O_2 cannot be produced by catalyzing the decomposition of H_2O_2, as the result of the low concentration of H_2O_2 in the tumor microenvironment (< 50 mM) [93]. In addition to increasing the generation of oxygen, PDT can be indirectly enhanced by reducing the consumption of oxygen. Generally, more nutrition and energy are needed by abnormally proliferating cancer cells [94]. Accordingly, tumor cells are sensitive to the concentration of glucose, aerobic glycolysis donor [95]. Zhang's group prepared cancer targeted cascade bioreactor (designated as mCGP, which is mem@catalase@GOx@PCN-224) for synergistic starvation and PDT [96]. PCN-224 acted as a vehicle loading glucose oxidase (GOx) to decompose endogenous glucose and catalase to catalyze endogenous H_2O_2. The reduced consumption of oxygen and increased O_2 synergistically led to the improved cytotoxic $^1O_2$ production under the hypoxic microenvironment. Lactate, known as an energy source in tumor cells, is able to be absorbed by monocarboxylate transporter 1 (MCT1) and oxidized to provide ATP for cells surviving and growing [97]. Zhang's group incorporated α-cyano-4 hydroxycinnamate, an MCT1 inhibitor, into porous Zr(IV)-based porphyrin MOF nanoparticles to reduce lactate absorption [98]. In tumor cells, lactate-driven aerobic respiration was therefore converted to anaerobic glycolysis. The change of energy supply reduced oxygen consumption, which enhanced PDT effect for cancer cells. Chen's group designed a UMOFs@AuNPs nanoreactor for effective biocatalytic cascade driven PDT by integrating ultrasmall Au nanoparticles, upconversion nanoparticles (UCNPs), and zirconium/iron porphyrin MOF (Fig. 5c) [99]. In the tumor microenvironment, the ultrasmall AuNPs effectively depleted the glucose and produced a considerable amount of H_2O_2. The produced H_2O_2 was subsequently catalyzed by the catalase-like MOF to produce O_2. Upon NIR light irradiation, the emitted visible light from the UCNPs excited the iron porphyrin MOF to generate cytotoxic $^1O_2$. Synergistic cascade reaction driven PDT against solid tumors was achieved both in vitro and in vivo.

The elimination of singlet oxygen by reductive substances in cells can weaken the PDT effect [100]. PCN-222 served not only as PDT agent but also as the carrier of alkaloid piperlongumine (PL), a thioredoxin reductase (TrxR) inhibitor used to block the ROS elimination pathway (Fig. 5d) [101]. The combination of PDT and PL caused promotions of ROS level about 1.6 times, cytotoxicity about two times and apoptosis rate about three times higher than traditional PDT alone. Tang's group reported a Cu (II)-metalated nMOF for PDT using Cu (II) as an active center [102]. Intracellular GSH was specifically bounded and absorbed by Cu(II) center, thus the ROS level was increased directly. Breast cancer treatment in mice with MOF-2 indicated comparable therapeutic effects with the commercially anticancer drug camptothecin (CPT). Recently, Jiang's group revealed a new mechanism of $^1O_2$ production without oxygen and light that overcame the reduced PDT efficiency caused by a high GSH level [103]. The ultrathin two-dimensional Cu-TCPP nanosheets decreased the intracellular GSH by cyclic conversion of Cu^{2+} and Cu^+ to avoid consuming $^1O_2$. TCPP ligands were peroxidized under weak acid tumor microenvironment and excessive H_2O_2. Meanwhile, Cu-TCPP nanosheets with peroxidase-like nanozyme activity reduced peroxidized TCPP ligands to peroxyl radicals (ROO·) species with the help of trace Cu^{2+} ions. According to the Russell mechanism [104], $^1O_2$ was generated by the reaction of ROO· species spontaneous recombination without oxygen and light.

Photothermal therapy (PTT)

PTT is performed by converting near infrared light into heat for photothermal ablation of tumors. In recent years, PTT has become one of the effective cancer therapy strategies due to its non-invasiveness, safety, and few side-effects [105]. Inorganic nanomaterials (such as gold, copper sulfide and carbon nanomaterials) and organic materials (such as porphyrin, indocyanine green, and polypyrrole) are the familiar photothermal agents [106–109]. To achieve a better therapy effect at target tissues, photothermal agents are usually compounded with functional nanomaterials. For example, CuS nanoparticles were wrapped in ZIF-8 with a large loading rate and delivered into cancer cells, showing excellent photothermal therapeutic effects [110]. Tian's group prepared Au@MOFs core–shell nanoplatform for NIR hyperthermia via a green synthesis method, which demonstrated the high efficacy of photothermal therapy around the tumor site under an 808 nm laser (Fig. 6a) [111]. Among them, AuNRs acted as seeds for MOFs growth, and the porous Fe-(benzene-1,3,5-tricarboxylate)$_3$(H_2O)$_6$ shells prevented AuNRs from gathering. To reduce the potential biological toxicity caused by inorganic materials, uniform polypyrrole nanoparticles with good biodegradability have been selected for photothermal ablating tumors [109]. Chen's group embedded polydopamine into the pores of $Mn_3[Co(CN)_6]_2$ through one-pot method (Fig. 6b) [112]. The resultant polydopamine-MOFs hybrid nanogel nanoparticles (named MCP) exhibited a strong NIR absorption capacity for photothermal conversion. After modifying polyethylene glycol (PEG) and thiol terminal cyclic arginine-glycine-aspartate

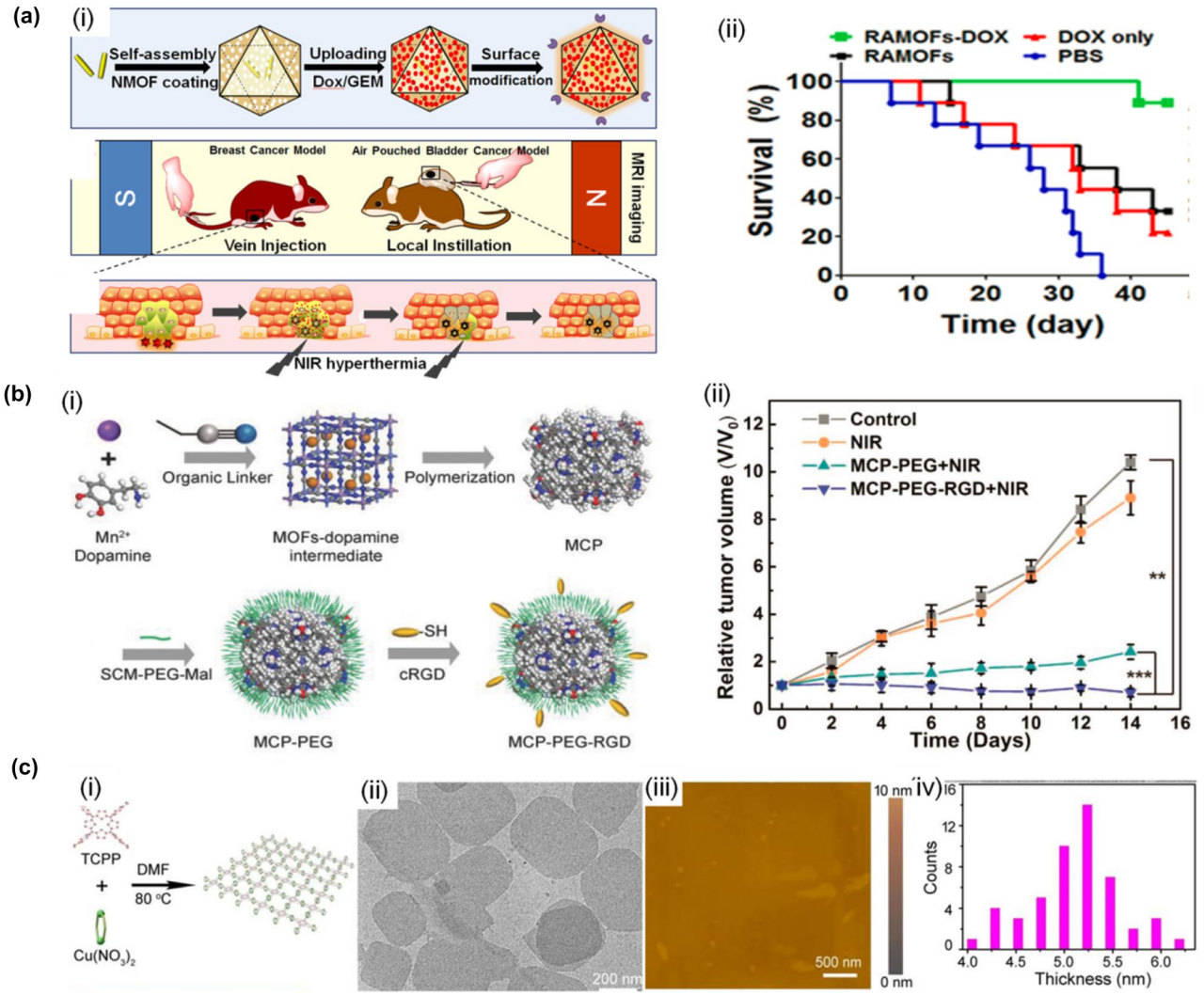

Fig. 6 Schematic illustration of the nMOFs as photothermal agents for photothermal therapy (PTT). **a** (i) Schematic illustration of the design and synthesis of nMOFs-drug platform, in vivo vein injection, and local instillation of the nMOFs-drug for tumor magnetic resonance imaging, and the combinatorial chemophotothermal therapy of tumor. (ii) Survival rates for breast cancer mice treated with RAMOFs-DOX, RAMOFs, DOX, and PBS (*RAMOF* RGD-Au@Fe-MOF, *DOX* doxorubicin, *PBS* phosphate buffered saline, 0.01 M, pH 7.2). Reproduced with permission [111]. Copyright 2020, American Chemical Society. **b** Schematic representation of the preparation of MCP, MCP-PEG, and MCP-PEG-RGD NPs (*NPs* nanoparticles, *MCP* the resultant hybrid NPs, *PEG* polyethylene glycol, *RGD* arginine-glycine-aspartic). (ii) In vivo PTT (photothermal therapy): tumor growth curves of mice after different treatments. Reproduced with permission [112]. Copyright 2018, John Wiley & Sons. **c** (i) Schematic illustration of the synthesis of Cu-TCPP (copper-tetrakis (4-carboxyphenyl) porphyrin) MOFs. (ii) transmission electron microscope (TEM) and (iii) Atomic force microscope (AFM) images of Cu-TCPP MOF nanosheets. (iv) Size histogram representing the thickness distribution of Cu-TCPP MOF nanosheets from AFM images. Reproduced with permission [113]. Copyright 2018, Ivyspring International Publisher

acid (cRGD-SH) peptides on the surface of MCP, the obtained MCP-PEG-RGD with uniform size distributions, increased long-term solution stability and biocompatibility enhanced tumor accumulation and broadened the application prospects for therapeutic nanoplatforms.

nMOFs are rarely used alone as photothermal agents because of the poor near infrared (NIR) absorption. Particularly, Wu's group reported an ultra-thin Cu-TCPP (copper-tetrakis (4-carboxyphenyl) porphyrin) nanosheets for photothermal therapy, in which Cu^{+} coexisted with Cu^{2+} led to the strong NIR absorption owing to the d-d energy band transition of Cu^{2+} (Fig. 6c) [113]. Compared to bulk materials, the two-dimensional nanosheets exhibited better photothermal properties allowing quick response to external light. Zhou's group reported a porphyrin MOF with a single atom Fe site (denoted as P-MOF) through adjusting band gap energy and UV–Vis absorption spectrum [87]. P-MOF with the narrow HOMO–LUMO gap and strong absorption

at 808 nm were potential for NIR-driven photothermal applications.

Other therapies

Chemodynamic therapy (CDT)

In the past decades, CDT with characteristics of selective treatment and low side effects, has been extensively investigated [114, 115]. In principle, CDT is driven by Fenton or Fenton-like reactions, producing cytotoxic hydroxyl radical (·OH) mediated by Fe^{3+}/Fe^{2+} redox pairs and H_2O_2 [115–117]. Especially, CDT does not require oxygen and external energy, which overcomes the shortcomings of PDT, less singlet oxygen generation under hypoxic conditions, and insufficient laser penetration depth. Compared to tumor cells with overexpressed H_2O_2, the breaking balance of intracellular redox/oxidation state can be avoided in normal cells [118].

nMOFs with customized structure, high loading rate, and modification capability can not only be directly used as catalysts for Fenton reaction but also enhance the application of CDT by loading molecules or surface modification [116, 119, 120]. Zhang's group reported that MIL-100 containing Fe^{3+} could generate •OH in the presence of H_2O_2 for CDT via Fenton-like reaction (Fig. 7a) [121]. Hyaluronic acid (HA) was modified on the surface of MIL-100 to improve the dispersibility and targeting ability towards tumor tissues. Relative to sluggish activity of Fe^{3+}, ferrocene (Fc) composed of Fe^{2+} showed a faster Fenton reaction rate in the physiological environment, and ferrocene (Fc) had received widespread attention due to its high stability, low toxicity, and reversible redox properties [122–124]. Han's group synthesized Co-Fc nMOF incorporating glucose oxidase (GOx) to promote the generation of cytotoxic hydroxyl radicals in

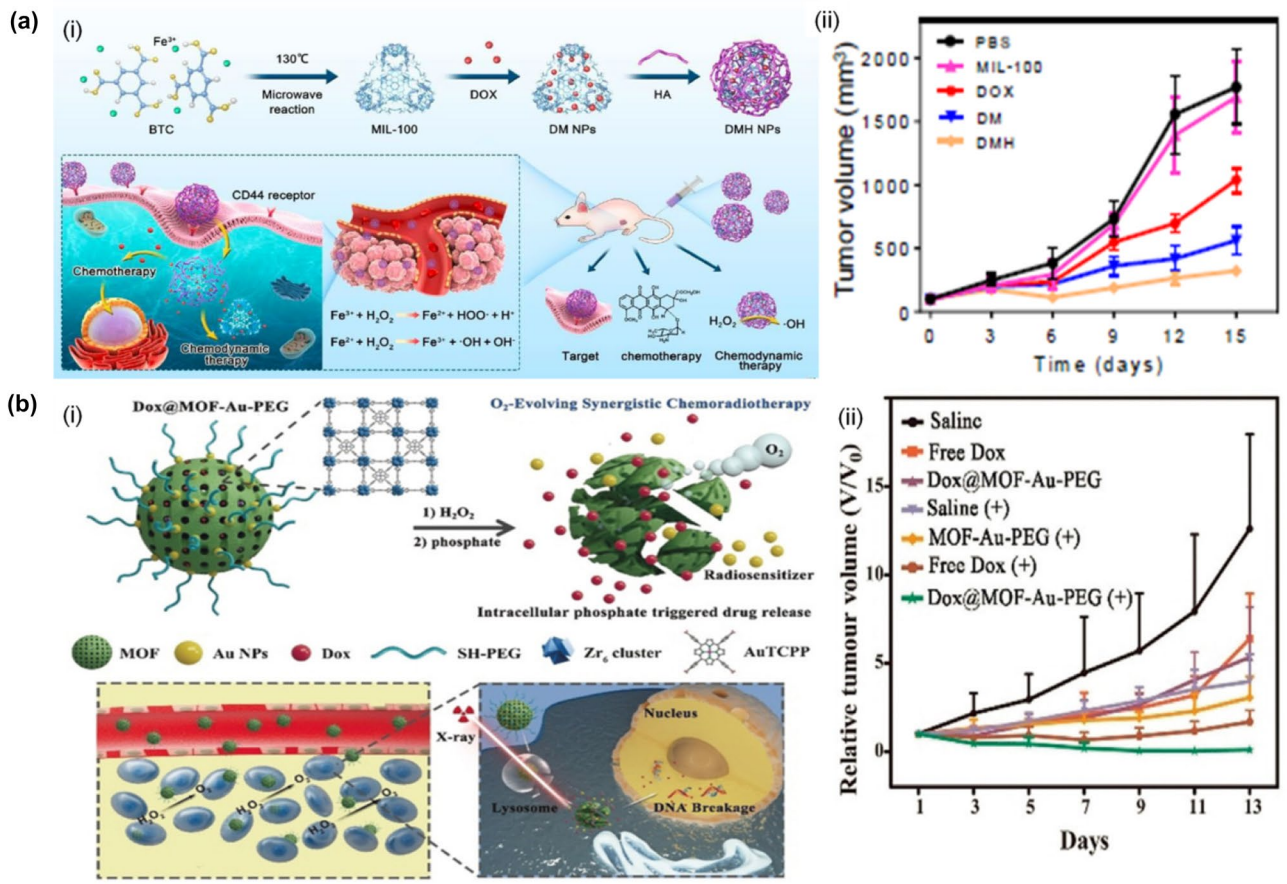

Fig. 7 Schematic illustration of the nMOFs as nanocarriers for chemodynamic therapy (CDT) and radiotherapy (RT). **a** (i) Schematic illustration of the preparation and application of DMH NPs (*DMH* modified hyaluronic acid on the surface of MIL-100 loading doxorubicin, *MIL* Materials of Institute Lavoisier). (ii) The tumor growth curves of mice treated with PBS, MIL-100, DOX, DM, DMH (*DOX* doxorubicin, *DM* MIL-100 loading doxorubicin). Reproduced with permission [121]. Copyright 2019, Royal Society of Chemistry. **b** (i) Schematic representation showing the main components of DOX@MOF-Au-PEG (*PEG* polyethylene glycol) and the mechanism of O2 self-supplying synergistic chemoradiotherapy. (ii) Tumor growth curves of the mice administered with different treatments. Reproduced with permission [35]. Copyright 2019, John Wiley & Sons

tumor cells [125]. Endogenous glucose was catalyzed by GOx and the productions, gluconic acid, and H_2O_2, provided a more compatible microenvironment for Fenton-like reaction. Qiao's group reported a novel CDT agent through conjugating iron MOF nanoparticles and folic acid, named MOF-FA [126]. MOF-FA was completely stable at neutral pH, while in weak acid conditions, iron ions were released to form MOF-FA and catalyzed H_2O_2 to generate ·OH via Fenton reaction.

Radiotherapy (RT)

Relying on the interaction between ionizing radiations and tumor tissues, RT destroys the double-stranded DNA in tumor cells [127, 128]. The effectiveness of RT depends on the radio-sensitivity of tumor tissues, which is affected by proliferation, differentiation, and oxygen content of tumor cells [129]. Thus, the low ionizing radiation energy absorption rate and hypoxia microenvironment of tumor cells have limited the radiation therapeutic effect. To promote RT sensitivity, increasing the tumor oxygen content and introducing radiation sensitizers are effective strategies [130]. Meng's group proposed a quercetin-modified Zr-MOF nanoparticle (Zr-MOF-quercetin) as a versatile radiotherapy material [131]. Quercetin acted as a radiosensitizer to enhance the absorption of radiant energy. Besides, carbonic anhydrase IX (CA IX), one of the causes of hypoxia in tumor cells, was inhibited via the combination of Zn^{2+} and 1,4-phthalic acid released from decomposed Zr-MOF in an acidic environment. Thus, this biodegradable nanomaterial simultaneously increased the radiant energy absorption and improved the tumor hypoxia environment, resulting in enhanced RT effect. In addition to traditional sensitizer compounds, metal atoms with high plateau atomic numbers and large X-ray energy attenuation coefficients, such as Au, Hf, and Ta, are also ideal radiation sensitizers [132–134]. Chen's group in situ synthesized AuNPs on the surface of MOFs that acted as drug container (Fig. 7b) [35]. Decorated AuNPs served as an effective radiosensitizer and stabilized the nanocomposite against premature degradation during blood circulation. Moreover, the prepared MOF-Au hybrid worked as an artificial enzyme and catalyzed endogenous H_2O_2 into O_2, which was beneficial to O_2-dependent RT efficiency.

Combined therapy

Compared with homogenous cancer treatment methods, adopting combination therapies of two or more treatment methods has cumulative or even higher anti-cancer efficacy, which can reduce drug dose, toxicity, and side effects, and can also overcome potential drug resistance. However, directly mixing different functional materials together are complicated, or even, the primary therapeutic effect would be weakened. Therefore, it is necessary to develop simple, low-cost, and synergistic multifunctional nano-therapy platforms.

The combination of PTT and PDT has revealed various advantages in improving the efficiency of cancer treatment [135–137]. The heat generated during the PTT process can improve the oxygen supply and then ease the limitation of hypoxia in the PDT process. Lei's group encapsulated the black quantum dots inside the MIL-type MOF for photodynamic-thermal synergistic therapy both in vivo and in vitro [91]. Quantum dots exhibited excellent photothermal conversion efficiency and singlet oxygen production efficiency owing to the quantum confinement and edge effects. Zhou's group reported a type of P-MOF containing porphyrin MOF with single atom Fe site for photodynamic-thermal combination therapy under 808 nm irradiation [138]. The narrow band-gap energy (1.31 eV) of P-MOF enhanced NIR photons absorption for PTT. In addition, the conversion of the spin state of Fe(III) in P-MOF promoted the generation of $^1O_2$ for PDT. Dong's group synthesized zirconium-ferriporphyrin MOF (Zr-FeP MOF) nanoshuttles with inherent photothermal conversion efficiency and high photothermal conversion efficiency (Fig. 8a) [139]. The introduction of heat shock protein 70 (Hsp70) into the porous Zr-FeP MOF realized low-temperature PTT and reduced damage to normal tissues. Under single near-infrared laser irradiation, the tumor growth was effectively suppressed both in vitro and in vivo.

Acting as the intelligent DDS, nMOFs have overcome the shortcomings of using chemotherapy drugs alone. To inhibit the growth of tumor cells more effectively, researchers have investigated the synergistic effect of chemotherapy and phototherapy which has demonstrated excellent anticancer capabilities. A dual-function nanoprobe was fabricated through noncovalent loading camptothecin (Cam) into NH_2-MIL-101(Fe) and covalent modifying chlorine e 6 (Ce_6)-labeled cathepsin B (CaB) substrate peptide on the surface [140]. Over expressed CaB in tumor cells cut off substrate peptide and then Ce_6 and Cam diffused in the cytoplasm for PDT and chemotherapy, respectively. Compared with 3D nMOFs, the 2D nMOFs nanosheets possessed significantly higher drug carrying capacity and higher light-excited singlet oxygen production efficiency, which was attributed to the unique larger surface area [141]. Wu's group developed a core–shell nano-system for both redox-responsive DOX releasing and PDT taking advantage of redox responsive selenium (Se) substituted polymer as the shell and photosensitive MOF as the core [142]. Under single light irradiation, singlet oxygen was produced from the inner core and then cracked the shell polymer to release DOX for chemotherapy. Moreover, Liu's group developed a nanotherapeutic delivery system for combinatorial

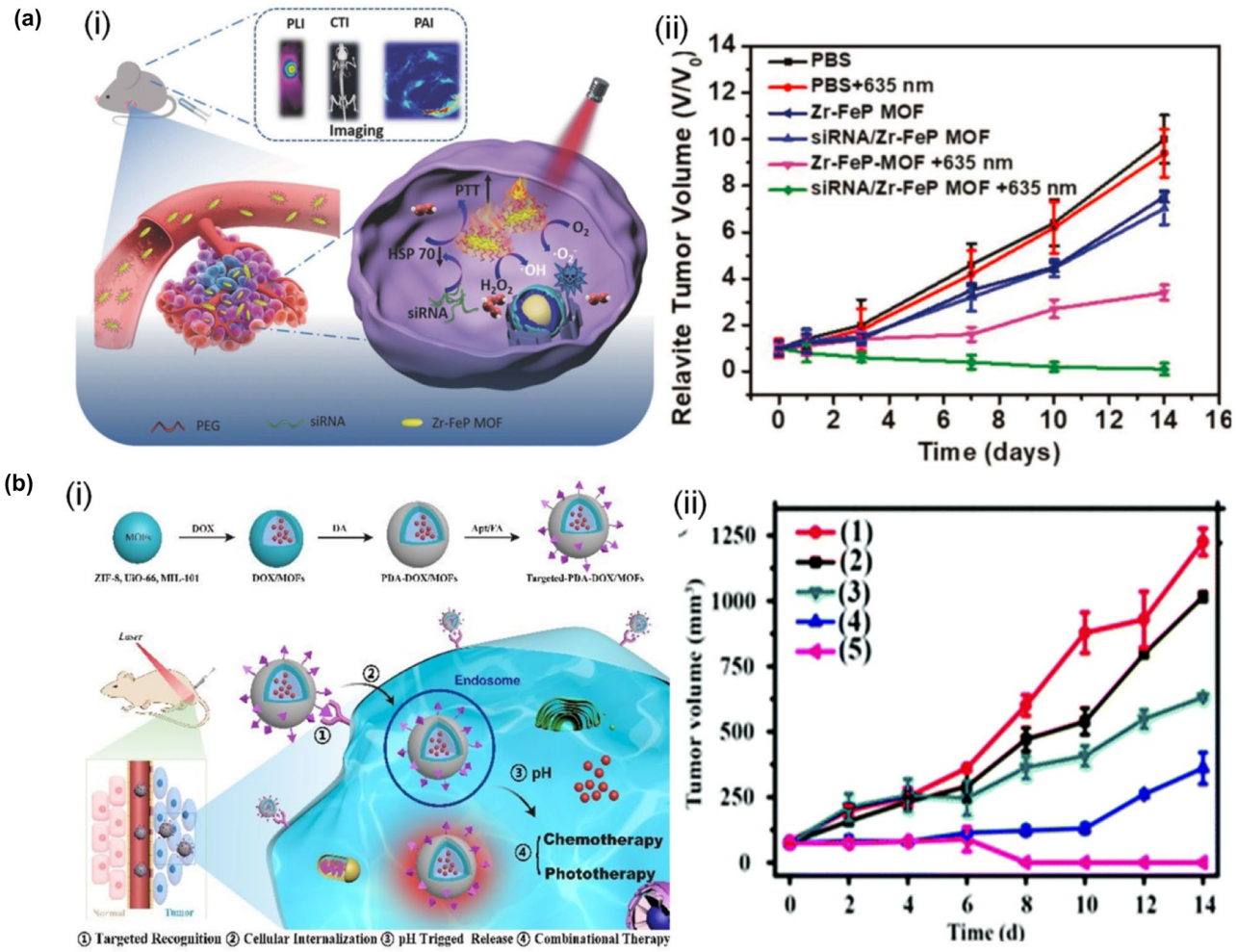

Fig. 8 Schematic illustration of the nMOFs as nanocarriers for photodynamic-thermal combinational therapy and chemo-photothermal combinational therapy respectively. **a** (i) Schematic illustration of siRNA/Zr-FeP MOF (*Zr-FeP MOF* zirconium-ferriporphyrin metal–organic framework) nanoshuttles for multimode imaging diagnosis and combination of low-temperature PTT and PDT (*PTT* photothermal therapy, *PDT* photodynamic therapy) for cancer treatment. Reproduced with permission [139]. Copyright 2018, John Wiley & Sons. **b** (i) Schematic illustration of the stimuli-responsive multifunctional MOFs as an efficient nanocarriers for targeted drug delivery and combinational therapy. (ii) Tumor related volume following treatment with (1) PBS, (2) aptamer-polydopamine/ZIF-8 (*ZIF* zeolitic imidazolate frameworks), (3) aptamer-polydopamine/ZIF-8 with 808 nm irradiation, (4) aptamer-polydopamine-doxorubicin/ZIF-8, (5) aptamer-polydopamine-doxorubicin/ZIF-8 with 808 nm irradiation. Reproduced with permission [143]. Copyright 2019, Royal Society of Chemistry

chemo-photothermal therapy (Fig. 8b) [143]. ZIF-8 acted as DOX carrier and polydopamine with excellent photothermal conversion efficiency realized heat treatment under light.

There are other combined therapy methods. A MIL-100-based nano-platform for combining chemotherapy and chemodynamic tumor therapy was reported [121, 144]. As the metal center of MIL-100, Fe^{3+} generated ·OH via a Fenton-like reaction in the presence of H_2O_2. At the same time, MIL-100 served as a drug carrier with high DOX loading efficiency for chemotherapy. The combined therapy effectively induced MCF-7 cell death and exhibited preferable tumor suppression. Chen's group prepared hybrid nanoparticles with excellent anti-cancer efficacy and negligible systemic toxicity via decorating porphyrin MOFs with AuNPs [35]. The synergistic effect of radiotherapy and chemotherapy was attributed to the radiosensitizing effect of AuNPs and DOX encapsulated in MOF scaffold, respectively. Besides, the increasing tumor oxygen caused by catalase-like activity of nanohybrid further enhanced chemoradiation. Lin's group integrated Ru-based photosensitizers into the nMOF and synthesized Hf-DBB-Ru for mitochondrial targeted and X-ray activated cancer treatment for the first time (Fig. 9a) [145]. Hf-DBB-Ru with cationic UiO topology had strong mitochondrial targeting properties. Upon X-ray irradiation, Hf_6 secondary building units (SBUs) played a role in radiotherapy by absorbing X-rays

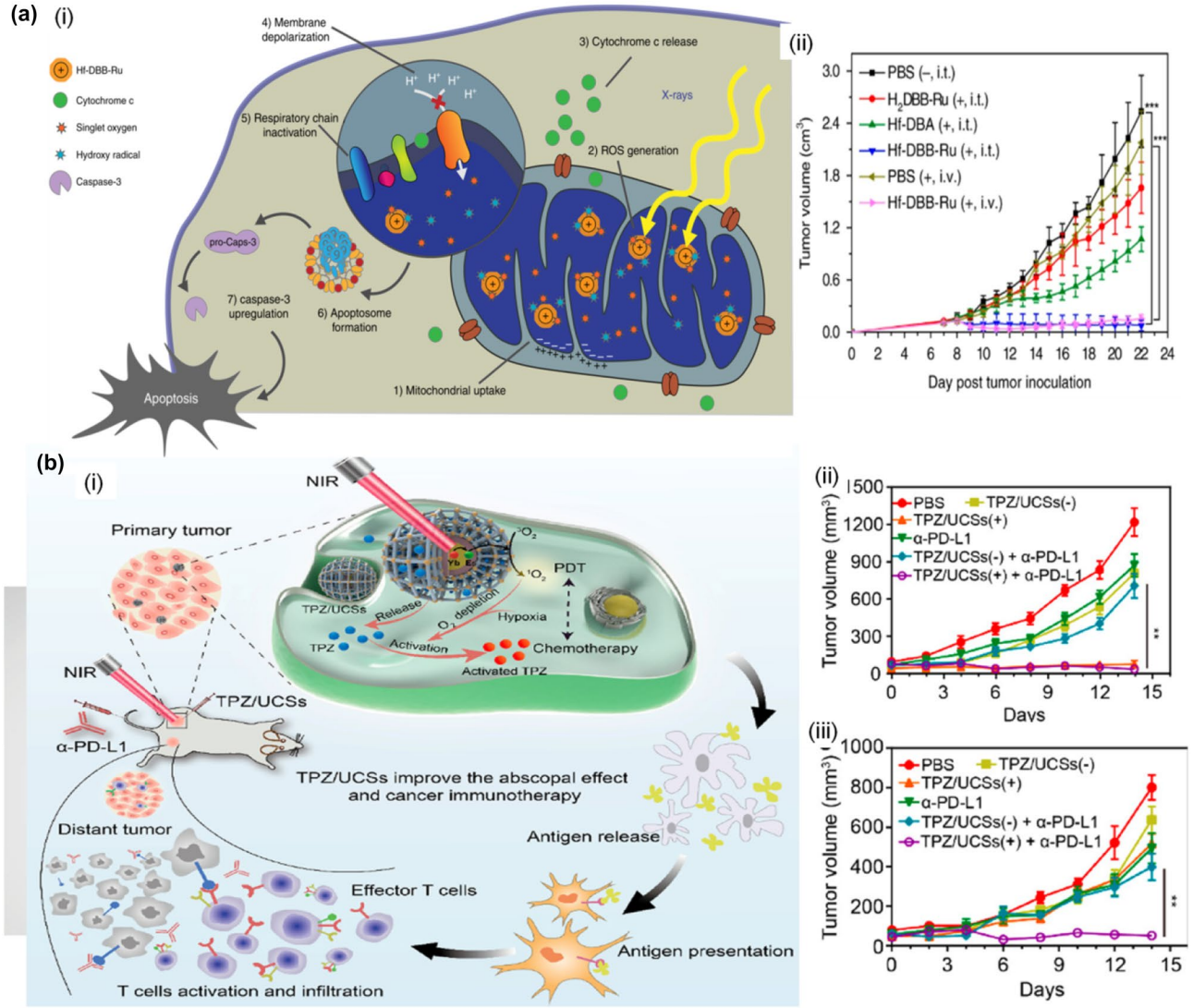

Fig. 9 Schematic illustration of the nMOFs as nanocarriers for radiotherapy–radiodynamic combinational therapy and PDT-chemotherapy combinational therapy. **a** (i) Schematic showing the RT and RDT process enabled by Hf-DBB-Ru and mitochondria-targeted RT-RDT mediated by Hf-DBB-Ru (*RT* radiotherapy, *RDT* radiodynamic therapy, *DBB-Ru* bis(2,2′-bipyridine)(5,5′-di(4-benzoato)-2,2′-bipyridine) ruthenium (II) chloride). (ii) Tumor growth inhibition/regression curves in tumor-bearing mice with different treatments. Reproduced with permission [145]. Copyright 2018, Springer Nature. **b** (i) Schematic illustration of the structure of TPZ/UCSs (*TPZ* tirapazamine, *UCSs* upconversion nanoparticle@porphyrinic MOFs) and their application for tumor treatment through the combination of NIR light-triggered PDT (*NIR* near infrared, *PDT* photodynamic therapy) and hypoxia-activated chemotherapy with immunotherapy. Tumor growth of (ii) primary tumors and (iii) distant tumors in tumor-bearing mice with different treatments. Reproduced with permission [147]. Copyright 2020, American Chemical Society

prior to tissues and generating hydroxyl radicals. Then the energy was transferred to $Ru(bpy)_3^{2+}$ ligands to generate singlet oxygen. The radiotherapy–radiodynamic therapy process depolarized the mitochondrial membrane potential and released cytochrome c to initiate tumor cell apoptosis.

Yao's group constructed a multifunctional nMOFs system including hypoxia inducible factor signaling inhibitor and immunologic adjuvant (CpG) [146]. After photodynamic therapy, the aggravation of hypoxic survival signaling was blocked by signaling inhibitor to inhibit survival and metastasis. Meanwhile, antitumor immune responses were initiated with the help of CpG adjuvant to eliminate residue cancer cells. The synergistical strategy significantly boosted cancer treatment efficiency in vitro and in vivo which was expected for future clinical treatment. Li's group prepared the upconversion nanoparticles@porphyrinic MOFs core–shell heterostructure with an efficiently loading rate for the combinational therapy of NIR light-triggered PDT and hypoxia-activated chemotherapy against hypoxic tumors (Fig. 9b) [147]. Upconversion nanoparticle (UCNPs)

Table 1 The nMOFs based nanoplatforms for cancer therapy

MOF	Release mechanism	For cancer therapy	Refs.
UiO-66	Amorphization	Chemotherapy	[42]
γ-CD-MOF	pH	Chemotherapy	[45]
CCM@MOF-M(DTBA)	GSH	Chemotherapy	[50]
ZJU-801	Naphthalene moiety	Chemotherapy	[59]
UMOFs@AuNPs	NIR	PDT	[86]
Cu (II)-metalated nMOF	GSH	PDT	[89]
RGD-Au@Fe-MOF	NIR	PTT	[98]
MCP	NIR	PTT	[99]
MOF-FA	pH	CDT	[113]
Zr-MOF-quercetin	pH	RT	[118]

converted NIR light into UV/Vis light to stimulate the generation of ROS due to the energy transfer from UCNPs core to MOFs shell. The loaded hypoxia-activatable prodrug (tirapazamine, TPZ) caused obvious cell damage in hypoxic environment. Furthermore, anti-programmed death ligand 1 (α-PD-L1) treatment cooperating with the nanoplatform promoted the abscopal effect by generating specific cytotoxic T cell tumor infiltration, thereby completely inhibiting the growth of untreated distant tumors.

Researchers have proved that nMOFs are prospective nanomaterials for traditional cancer therapies such as chemotherapy and radiotherapy. The novel design strategies have overcome the problem of low therapy effect and low selectivity. Even for increasing types of new cancer therapies, nMOFs also exhibited their broad and excellent prospect for biomedical applications.

Conclusion and outlook

In summary, we briefly summarize the latest biomedical development of nMOFs acting as anti-cancer therapeutic agents. Table 1 is listed to present the representative examples of nMOFs based nanoplatforms for cancer therapy. For precise cancer diagnosis and timely therapy, nMOFs have already emerged in many nanomaterials due to their outstanding characteristics including tunable structures and morphologies, large specific surface area, high porosities and loading rates, and variable affinities. The sizes, topologies, and surface properties of nMOFs can be adjusted by changing the metal center and organic ligands, and these physical properties affect the inherent biocompatibility and biotoxicity of nMOFs. Thus more toxicity studies for synthesizing biocompatible nMOFs with suitable structure and size is in urgent need. A large specific area, high porosity, and uniform pore size contribute to nMOFs acting as nanocarriers to load sensing, imaging, or therapy agents with high loading rates. In addition, the agents can be immobilized more firmly due to the customizable functional groups on the nMOFs surface. The functional agents can be directly assembled as a part of nMOFs, which can not only avoid the adverse reactions caused by the aggregation of functional agents, but also act as multifunctional nano-platform bringing bioimaging and therapy.

However, to complete the conversion from the workbench to the clinic, there are still some challenges need to be overcome. First, the accumulation of biocompatibility and toxicity data is a key factor for nMOFs converting into clinic. The accumulation and decomposition of nMOFs in vivo may cause potential biological toxicity. Thus the toxicity and long-term effects of nMOFs have to be investigated in vivo to be fully characterize, however they are mostly done in vitro when considering most of the current safety investigations have examined only the cell lines. To with this, a comprehensive assessment of various nMOFs' acute and long-term toxicity is quite essential for biomedical applications, especially of both the metals and the organic building blocks. Second, how to enhance the stability of nMOFs under physiological conditions to avoid the rapid degradation, the unexpected aggregation, or the ineffectiveness in vitro and in vivo is another challenge. Although many efforts have been made to test and evaluate the nMOFs' stability in water, the results under physiological conditions are still limited. Third, targeted degradation of nMOFs is expected for the drug delivery in clinical trials. Differential degradation rate may be achieved by exploring the nMOFs' degradation mechanisms with composition of different metal ions and organic compounds in further study.

In conclusion, nMOFs have attracted wide attention owing to their unique characteristics as well as excellent performances. The design and fabrication of multi-functional biomedical platforms using MOFs and their ability, toxicity, and targeting ability in vitro/vivo remains challengeable yet has innovative prospects [39, 40, 148–155]. Nonetheless, there is a long way for applying the biocompatible nMOFs in cancer therapy with biological safety and good effectiveness. For all that, more efforts put in achieving breakthrough in developing nMOFs-based platforms for treatments of human cancers are encouraged. It is expected that nMOFs will play increasingly important roles in biomedical fields including biosensors, clinical diagnosis, and diseases therapy.

Acknowledgements This work was supported by grants from the National Natural Science Foundation of China (22022412, 21874155, 22104060), the Natural Science Foundation of Jiangsu Province (BK20200716, BK20191316), the Natural Science Foundation of the Jiangsu Higher Education Institutions of China (20KJB150019), Innovation and Entrepreneurship Doctor Program of Jiangsu Province

(JSSCBS20210317), the State Key Laboratory of Analytical Chemistry for Life Science (SKLACLS2106), and the Qing-Lan Project of Jiangsu Province (2019).

Declarations

Conflict of interest All authors have given approval to the final version of the manuscript. There is no conflict of interest to report.

References

1. Coussens, L.M., Werb, Z.: Inflammation and cancer. Nature **420**, 860–867 (2002)
2. Zhang, C., Zhao, Y., Xu, X., Xu, R., Li, H., Teng, X., Du, Y., Miao, Y., Lin, H.C., Han, D.: Cancer diagnosis with DNA molecular computation. Nat. Nanotechnol. **15**, 709–715 (2020)
3. Li, H., Eddaoudi, M., O'Keeffe, M., Yaghi, O.M.: Design and synthesis of an exceptionally stable and highly porous metal-organic framework. Nature **402**, 276–279 (1999)
4. Jin, R.H., Liu, Z.N., Liu, T., Yuan, P.Y., Bai, Y.K., Chen, X.: Redox-responsive micelles integrating catalytic nanomedicine and selective chemotherapy for effective tumor treatment. Chin. Chem. Lett. **32**, 3076–3082 (2021)
5. Yang, J., Dai, D.H., Ma, L.J., Yang, Y.W.: Molecular-scale drug delivery systems loaded with oxaliplatin for supramolecular chemotherapy. Chin. Chem. Lett. **32**, 729–734 (2021)
6. Anbia, M., Faryadras, M.: In situ Na center dot Cu-3(BTC)(2) and Li center dot Cu-3(BTC)(2) nanoporous MOFs synthesis for enhancing H-2 storage at ambient temperature. J. Nanostruct. Chem. **5**, 357–364 (2015)
7. Yang, L.M., Gao, P., Huang, Y.L., Lu, X., Chang, Q., Pan, W., Li, N., Tang, B.: Boosting the photodynamic therapy efficiency with a mitochondria-targeted nanophotosensitizer. Chin. Chem. Lett. **30**, 1293–1296 (2019)
8. Ghiamaty, Z., Ghaffarinejad, A., Faryadras, M., Abdolmaleki, A., Kazemi, H.: Synthesis of palladium-carbon nanotube-metal organic framework composite and its application as electrocatalyst for hydrogen production. J. Nanostruct. Chem. **6**, 299–308 (2016)
9. Wu, R., Wang, H.Z., Hai, L., Wang, T.Z., Hou, M., He, D.G., He, X.X., Wang, K.M.: A photosensitizer-loaded zinc oxide-polydopamine core-shell nanotherapeutic agent for photodynamic and photothermal synergistic therapy of cancer cells. Chin. Chem. Lett. **31**, 189–192 (2020)
10. Rodriguez, S., Torres, F.G., Arroyo, J., Gonzales, K.N., Troncoso, O.P., López, D.: Synthesis of highly stable κ/ι-hybrid carrageenan micro- and nanogels via a sonication-assisted microemulsion route. Polym. Renew. Resour. **11**, 69–82 (2020)
11. Makvandi, P., Chen, M., Sartorius, R., Zarrabi, A., Ashrafizadeh, M., Dabbagh Moghaddam, F., Ma, J., Mattoli, V., Tay, F.R.: Endocytosis of abiotic nanomaterials and nanobiovectors: inhibition of membrane trafficking. Nano Today **40**, 101279 (2021)
12. Gulla, S., Lomada, D., Araveti, P.B., Srivastava, A., Murikinati, M.K., Reddy, K.R., Inamuddin, Reddy, M.C., Altalhi, T.: Titanium dioxide nanotubes conjugated with quercetin function as an effective anticancer agent by inducing apoptosis in melanoma cells. J. Nanostruct. Chem. **11**, 721–734 (2021)
13. Tabasi, H., Babaei, M., Abnous, K., Taghdisi, S.M., Saljooghi, A.S., Ramezani, M., Alibolandi, M.: Metal–polymer-coordinated complexes as potential nanovehicles for drug delivery. J. Nanostruct. Chem. (2021). https://doi.org/10.1007/s40097-021-00432-7
14. Eivazzadeh-Keihan, R., Maleki, A.: Design and synthesis of a new magnetic aromatic organo-silane star polymer with unique nanoplate morphology and hyperthermia application. J. Nanostruct. Chem. (2021). https://doi.org/10.1007/s40097-021-00401-0
15. Nasri, S., Ebrahimi-Hosseinzadeh, B., Rahaie, M., Hatamian-Zarmi, A., Sahraeian, R.: Thymoquinone-loaded ethosome with breast cancer potential: optimization, in vitro and biological assessment. J. Nanostruct. Chem. **10**, 19–31 (2020)
16. Kong, X.J., Ji, X.T., He, T., Xie, L.H., Zhang, Y.Z., Lv, H.Y., Ding, C.F., Li, J.R.: A green-emission metal-organic framework-based nanoprobe for imaging dual tumor biomarkers in living cells. ACS Appl. Mater. Inter. **12**, 35375–35384 (2020)
17. Ma, M.Y., Lu, L.Y., Li, H.W., Xiong, Y.Z., Dong, F.P.: Functional metal organic framework/SiO_2 nanocomposites: from versatile synthesis to advanced applications. Polymers **11**, 1823 (2019)
18. Liu, P., Liu, X.J., Cheng, Y., Zhong, S.H., Shi, X.Y., Wang, S.F., Liu, M., Ding, J.S., Zhou, W.H.: Core-shell nanosystems for self-activated drug-gene combinations against triple-negative breast cancer. ACS Appl. Mater. Inter. **12**, 53654–53664 (2020)
19. Shu, Y., Lu, Q., Yuan, F., Tao, Q., Jin, D.Q., Yao, H., Xu, Q., Hu, X.Y.: Stretchable electrochemical biosensing platform based on Ni-MOF composite/Au nanoparticle-coated carbon nanotubes for real-time monitoring of dopamine released from living cells. ACS Appl. Mater. Inter. **12**, 49480–49488 (2020)
20. Hu, X., Saravanakumar, K., Sathiyaseelan, A., Rajamanickam, V., Wang, M.H.: Cytotoxicity of aptamer-conjugated chitosan encapsulated mycogenic gold nanoparticles in human lung cancer cells. J. Nanostruct. Chem. (2021). https://doi.org/10.1007/s40097-021-00437-2
21. Rehman, Y., Copet, C., Morlando, A., Huang, X.F., Konstantinov, K.: Investigation of ROS scavenging properties and in vitro cytotoxicity of oxygen-deficient La_2O_{3-x} nanostructure synthesized by spray pyrolysis method. J. Nanostruct. Chem. **10**, 347–361 (2020)
22. Yang, P., Gai, S., Lin, J.: Functionalized mesoporous silica materials for controlled drug delivery. Chem. Soc. Rev. **41**, 3679–3698 (2012)
23. Tabasi, H., Babaei, M., Abnous, K., Taghdisi, S.M., Saljooghi, A.S., Ramezani, M., Alibolandi, M.: Metal-polymer-coordinated complexes as potential nanovehicles for drug delivery. J. Nanostruct. Chem. **11**, 501–526 (2021)
24. Xu, Q.Y., Tan, Z., Liao, X.W., Wang, C.: Recent advances in nanoscale metal-organic frameworks biosensors for detection of biomarkers. Chin. Chem. Lett. (2021). https://doi.org/10.1016/j.cclet.2021.06.015
25. Duman, F.D., Forgan, R.S.: Applications of nanoscale metal-organic frameworks as imaging agents in biology and medicine. J. Mater. Chem. B **9**, 3423–3449 (2021)
26. Zhang, S., Pei, X., Gao, H., Chen, S., Wang, J.: Metal-organic framework-based nanomaterials for biomedical applications. Chin. Chem. Lett. **31**, 1060–1070 (2020)
27. Rojas, S., Devic, T., Horcajada, P.: Metal organic frameworks based on bioactive components. J. Mater. Chem. B **5**, 2560–2573 (2017)
28. Castillo-Blas, C., Montoro, C., Platero-Prats, A.E., Ares, P., Amo-Ochoa, P., Conesa, J., Zamora, F.: The role of defects in the properties of functional coordination polymers. Adv. Inorg. Chem. **76**, 73–119 (2020)
29. Peng, L., Zhang, J.L., Li, J.S., Han, B.X., Xue, Z.M., Yang, G.Y.: Surfactant-directed assembly of mesoporous metal-organic framework nanoplates in ionic liquids. Chem. Commun. **48**, 8688–8690 (2012)

30. Zheng, W.Z., Hao, X.L., Zhao, L., Sun, W.Z.: Controllable preparation of nanoscale metal-organic frameworks by ionic liquid microemulsions. Ind. Eng. Chem. Res. **56**, 5899–5905 (2017)
31. Zhang, L.Y., Gao, Y., Sun, S.J., Li, Z.H., Wu, A.G., Zeng, L.Y.: pH-Responsive metal-organic framework encapsulated gold nanoclusters with modulated release to enhance photodynamic therapy/chemotherapy in breast cancer. J. Mater. Chem. B **8**, 1739–1747 (2020)
32. Zhang, L., Ma, X.N., Liang, H.B., Lin, H.H., Zhao, G.Y.: A non-enzymatic glucose sensor with enhanced anti-interference ability based on a MIL-53(NiFe) metal-organic framework. J. Mater. Chem. B **7**, 7006–7013 (2019)
33. Huang, X., Sun, X., Wang, W.L., Shen, Q., Tang, X.N., Shao, J.J.: Nanoscale metal-organic frameworks for tumor phototherapy. J. Mater. Chem. B **9**, 3756–3777 (2021)
34. Lei, B.Q., Wang, M.F., Jiang, Z.L., Qi, W., Su, R.X., He, Z.M.: Constructing redox-responsive metal–organic framework nanocarriers for anticancer drug delivery. ACS Appl. Mater. Interfaces **10**, 16698–16706 (2018)
35. He, Z.M., Huang, X., Wang, C., Li, X., Liu, Y., Zhou, Z., Wang, S., Zhang, F., Wang, Z., Jacobson, O., Zhu, J.J., Yu, G., Dai, Y., Chen, X.Y.: A catalase-like metal-organic framework nanohybrid for O_2-evolving synergistic chemoradiotherapy. Angew. Chem. Int. Ed. **58**, 8752–8756 (2019)
36. Su, Z.P., Ye, F.Y., He, K.Y., Yang, T., Li, W., Ren, J.L.: Determination of acetamiprid by fluorescence monitoring of a glycine-l-histidine copper-organic framework aptasensor. Anal. Lett. (2021). https://doi.org/10.1080/00032719.2021.1946555
37. Cai, H., Huang, Y.L., Li, D.: Biological metal-organic frameworks: Structures, host-guest chemistry and bio-applications. Coord. Chem. Rev. **378**, 207–221 (2019)
38. Zhu, H.L., Liu, D.X.: The synthetic strategies of metal-organic framework membranes, films and 2D MOFs and their applications in devices. J. Mater. Chem. A **7**, 21004–21035 (2019)
39. He, L.C., Liu, Y., Lau, J., Fan, W.P., Li, Q.Y., Zhang, C., Huang, P.T., Chen, X.Y.: Recent progress in nanoscale metal-organic frameworks for drug release and cancer therapy. Nanomedicine **14**, 1343–1365 (2019)
40. Zhou, J., Tian, G., Zeng, L., Song, X., Bian, X.: Nanoscaled metal-organic frameworks for biosensing, imaging, and cancer therapy. Adv. Healthc. Mater. **7**, 1800022 (2018)
41. Zhang, W., Mao, J.H., Zhu, W., Jain, A.K., Liu, K., Brown, J.B., Karpen, G.H.: Centromere and kinetochore gene misexpression predicts cancer patient survival and response to radiotherapy and chemotherapy. Nat. Commun. **7**, 12619 (2016)
42. Ren, H., Zhang, L., An, J., Wang, T., Li, L., Si, X., He, L., Wu, X., Wang, C., Su, Z.: Polyacrylic acid@zeolitic imidazolate framework-8 nanoparticles with ultrahigh drug loading capability for pH-sensitive drug release. Chem. Commun. **50**, 1000–1002 (2014)
43. Zhu, C.H., Peng, S.Q., Cui, L.L., Cao, W.Y., Zhang, L.S., Zhao, Z.M., Jia, L., Zhang, T.F., Guo, J.B., Pang, C.F.: Synergistic effects of rapamycin and fluorouracil to treat a gastric tumor in a PTEN conditional deletion mouse model. Gastric Cancer (2021). https://doi.org/10.1007/s10120-021-01229-x
44. Kiss, R.C., Xia, F., Acklin, S.: Targeting DNA damage response and repair to enhance therapeutic index in cisplatin-based cancer treatment. Int. J. Mol. Sci. **22**, 8199 (2021)
45. Zheng, D., Zhao, J.Y., Li, Y.C., Zhu, L.Y., Jin, M.C., Wang, L.Y., Liu, J., Lei, J.D., Li, Z.L.: Self-assembled pH-sensitive nanoparticles based on ganoderma lucidum polysaccharide-methotrexate conjugates for the co-delivery of anti-tumor drugs. ACS Biomater. Sci. Eng. **7**, 3764–3773 (2021)
46. Allen, T.M., Cullis, P.R.: Drug delivery systems: entering the mainstream. Science **303**, 1818–1822 (2004)
47. Sosnik, A., Menaker Raskin, M.: Polymeric micelles in mucosal drug delivery: challenges towards clinical translation. Biotechnol. Adv. **33**, 1380–1392 (2015)
48. Du, X.J., Wang, J.L., Liu, W.W., Yang, J.X., Sun, C.Y., Sun, R., Li, H.J., Shen, S., Luo, Y.L., Ye, X.D., Zhu, Y.H., Yang, X.Z., Wang, J.: Regulating the surface poly(ethylene glycol) density of polymeric nanoparticles and evaluating its role in drug delivery in vivo. Biomaterials **69**, 1–11 (2015)
49. Gong, P., Sun, L., Wang, F., Liu, X., Yan, Z., Wang, M., Zhang, L., Tian, Z., Liu, Z., You, J.: Highly fluorescent N-doped carbon dots with two-photon emission for ultrasensitive detection of tumor marker and visual monitor anticancer drug loading and delivery. Chem. Eng. J. **356**, 994–1002 (2019)
50. Wang, Y., Zhao, Q., Han, N., Bai, L., Li, J., Liu, J., Che, E., Hu, L., Zhang, Q., Jiang, T., Wang, S.: Mesoporous silica nanoparticles in drug delivery and biomedical applications. Nanomedicine **11**, 313–327 (2015)
51. Horcajada, P., Serre, C., Maurin, G., Ramsahye, N.A., Balas, F., Vallet-Regí, M., Sebban, M., Taulelle, F., Férey, G.: Flexible porous metal-organic frameworks for a controlled drug delivery. J. Am. Chem. Soc. **130**, 6774–6780 (2008)
52. Horcajada, P., Chalati, T., Serre, C., Gillet, B., Sebrie, C., Baati, T., Eubank, J.F., Heurtaux, D., Clayette, P., Kreuz, C., Chang, J.S., Hwang, Y.K., Marsaud, V., Bories, P.N., Cynober, L., Gil, S., Férey, G., Couvreur, P., Gref, R.: Porous metal-organic-framework nanoscale carriers as a potential platform for drug delivery and imaging. Nat. Mater. **9**, 172–178 (2010)
53. Cai, G., Jiang, H.: A modulator-induced defect-formation strategy to hierarchically porous metal-organic frameworks with high stability. Angew. Chem. Int. Ed. **56**, 563–567 (2017)
54. Wang, Y., Yan, J., Wen, N., Xiong, H., Cai, S., He, Q., Hu, Y., Peng, D., Liu, Z., Liu, Y.: Metal-organic frameworks for stimuli-responsive drug delivery. Biomaterials **230**, 119619 (2020)
55. Orellana-Tavra, C., Baxter, E.F., Tian, T., Bennett, T.D., Slater, N.K.H., Cheetham, A.K., Fairen-Jimenez, D.: Amorphous metal-organic frameworks for drug delivery. Chem. Commun. **51**, 13878–13881 (2015)
56. Teplensky, M.H., Fantham, M., Peng, L., Wang, T.C., Mehta, J.P., Young, L.J., Moghadam, P.Z., Hupp, J.T., Farha, O.K., Kaminski, C.F., Fairen-Jimenez, D.: Temperature treatment of highly porous zirconium-containing metal–organic frameworks extends drug delivery release. J. Am. Chem. Soc. **139**, 7522–7532 (2017)
57. Wang, X., Chen, X.Z., Alcântara, C.C.J., Sevim, S., Hoop, M., Terzopoulou, A., de Marco, C., Hu, C., de Mello, A.J., Falcaro, P., Furukawa, S., Nelson, B.J., Puigmartí-Luis, J., Pané, S.: MOFBOTS: metal–organic-framework-based biomedical microrobots. Adv. Mater. **31**, 1901592 (2019)
58. Liang, Z., Yang, Z., Yuan, H., Wang, C., Qi, J., Liu, K., Cao, R., Zheng, H.: A protein@metal-organic framework nanocomposite for pH-triggered anticancer drug delivery. Dalton Trans. **47**, 10223–10228 (2018)
59. Jia, Q., Li, Z., Guo, C., Huang, X., Song, Y., Zhou, N., Wang, M., Zhang, Z., He, L., Du, M.: A γ-cyclodextrin-based metal-organic framework embedded with graphene quantum dots and modified with PEGMA via SI-ATRP for anticancer drug delivery and therapy. Nanoscale **11**, 20956–20967 (2019)
60. Kahn, J.S., Freage, L., Enkin, N., Garcia, M.A.A., Willner, I.: Stimuli-responsive DNA-functionalized metal-organic frameworks (MOFs). Adv. Mater. **29**, 1602782 (2017)
61. Mura, S., Nicolas, J., Couvreur, P.: Stimuli-responsive nanocarriers for drug delivery. Nat. Mater. **12**, 991–1003 (2013)
62. Liu, Y., Gong, C.S., Dai, Y., Yang, Z., Yu, G., Liu, Y., Zhang, M., Lin, L., Tang, W., Zhou, Z., Zhu, G., Chen, J., Jacobson, O., Kiesewetter, D.O., Wang, Z., Chen, X.: In situ polymerization on nanoscale metal-organic frameworks for enhanced

physiological stability and stimulus-responsive intracellular drug delivery. Biomaterials **218**, 119365 (2019)
63. Min, H., Wang, J., Qi, Y., Zhang, Y., Han, X., Xu, Y., Xu, J., Li, Y., Chen, L., Cheng, K., Liu, G., Yang, N., Li, Y., Nie, G.: Biomimetic metal–organic framework nanoparticles for cooperative combination of antiangiogenesis and photodynamic therapy for enhanced efficacy. Adv. Mater. **31**, 1808200 (2019)
64. Ranji-Burachaloo, H., Reyhani, A., Gurr, P.A., Dunstan, D.E., Qiao, G.G.: Combined fenton and starvation therapies using hemoglobin and glucose oxidase. Nanoscale **11**, 5705–5716 (2019)
65. Kim, K., Lee, S., Jin, E., Palanikumar, L., Lee, J.H., Kim, J.C., Nam, J.S., Jana, B., Kwon, T.H., Kwak, S.K., Choe, W., Ryu, J.H.: MOF × biopolymer: collaborative combination of metal-organic framework and biopolymer for advanced anticancer therapy. ACS Appl. Mater. Interfaces **11**, 27512–27520 (2019)
66. Yang, X., Tang, Q., Jiang, Y., Zhang, M., Wang, M., Mao, L.: Nanoscale ATP-responsive zeolitic imidazole framework-90 as a general platform for cytosolic protein delivery and genome editing. J. Am. Chem. Soc. **141**, 3782–3786 (2019)
67. Chen, W.H., Yu, X., Liao, W.C., Sohn, Y.S., Cecconello, A., Kozell, A., Nechushtai, R., Willner, I.: ATP-responsive aptamer-based metal-organic framework nanoparticles (NMOFs) for the controlled release of loads and drugs. Adv. Funct. Mater. **27**, 1702102 (2017)
68. Ma, Y., Li, X., Li, A., Yang, P., Zhang, C., Tang, B.: H_2S-activable MOF nanoparticle photosensitizer for effective photodynamic therapy against cancer with controllable singlet-oxygen release. Angew. Chem. Int. Ed. **56**, 13752–13756 (2017)
69. Cheung, T.W., Li, L.: Development of self-care textile wearables with thermally stimulated drug delivery function via biological and physical investigations. Text. Res. J. **91**, 820–827 (2021)
70. Fernandez, M., Orozco, J.: Advances in functionalized photosensitive polymeric nanocarriers. Polymers **13**, 2464 (2021)
71. Wu, L.J., Gao, S.Y., Zhao, T.L., Tian, K., Zheng, T.Y., Zhang, X.Y., Xiao, L.Y., Ding, Z.Z., Lu, Q., Kaplan, D.L.: Pressure-driven spreadable deferoxamine-laden hydrogels for vascularized skin flaps dagger. Biomater. Sci. **9**, 3162–3170 (2021)
72. Jiang, K., Zhang, L., Hu, Q., Zhang, Q., Lin, W., Cui, Y., Yang, Y., Qian, G.: Thermal stimuli-triggered drug release from a biocompatible porous metal–organic framework. Chem. Eur. J. **23**, 10215–10221 (2017)
73. Roth Stefaniak, K., Epley, C.C., Novak, J.J., McAndrew, M.L., Cornell, H.D., Zhu, J., McDaniel, D.K., Davis, J.L., Allen, I.C., Morris, A.J., Grove, T.Z.: Photo-triggered release of 5-fluorouracil from a MOF drug delivery vehicle. Chem. Commun. **54**, 7617–7620 (2018)
74. Lin, C., He, H., Zhang, Y., Xu, M., Tian, F., Li, L., Wang, Y.: Acetaldehyde-modified-cystine functionalized Zr-MOFs for pH/GSH dual-responsive drug delivery and selective visualization of GSH in living cells. RSC Adv. **10**, 3084–3091 (2020)
75. Li, Y., Jin, J., Wang, D., Lv, J., Hou, K., Liu, Y., Chen, C., Tang, Z.: Coordination-responsive drug release inside gold nanorod@metal-organic framework core–shell nanostructures for near-infrared-induced synergistic chemo-photothermal therapy. Nano Res. **11**, 3294–3305 (2018)
76. Ng, K.K., Zheng, G.: Molecular interactions in organic nanoparticles for phototheranostic applications. Chem. Rev. **115**, 11012–11042 (2015)
77. Yoon, I., Li, J., Shim, Y.K.: Advance in photosensitizers and light delivery for photodynamic therapy. Clin. Endosc. **46**, 7–23 (2013)
78. Lovell, J.F., Liu, T.W.B., Chen, J., Zheng, G.: Activatable photosensitizers for imaging and therapy. Chem. Rev. **110**, 2839–2857 (2010)
79. Agostinis, P., Berg, K., Cengel, K.A., Foster, T.H., Girotti, A.W., Gollnick, S.O., Hahn, S.M., Hamblin, M.R., Juzeniene, A., Kessel, D., Korbelik, M., Moan, J., Mroz, P., Nowis, D., Piette, J., Wilson, B.C., Golab, J.: Photodynamic therapy of cancer: an update. CA Cancer J. Clin. **61**, 250–281 (2011)
80. Chatterjee, D.K., Fong, L., Zhang, Y.: Nanoparticles in photodynamic therapy: an emerging paradigm. Adv. Drug Deliv. Rev. **60**, 1627–1637 (2008)
81. Dolmans, D.E.J.G., Fukumura, J.D., Jain, R.K.: Photodynamic therapy for cancer. Nat. Rev. Cancer **3**, 380–387 (2003)
82. Lismont, M., Dreesen, L., Wuttke, S.: Metal-organic framework nanoparticles in photodynamic therapy: current status and perspectives. Adv. Funct. Mater. **27**, 1606314 (2017)
83. Secret, E., Maynadier, M., Gallud, A., Chaix, A., Bouffard, E., Gary-Bobo, M., Marcotte, N., Mongin, O., El Cheikh, K., Hugues, V., Auffan, M., Frochot, C., Morère, A., Maillard, P., Blanchard-Desce, M., Sailor, M.J., Garcia, M., Durand, J.O., Cunin, F.: Two-photon excitation of porphyrin-functionalized porous silicon nanoparticles for photodynamic therapy. Adv. Mater. **26**, 7643–7648 (2014)
84. Konan, Y.N., Gurny, R., Allémann, E.: State of the art in the delivery of photosensitizers for photodynamic therapy. J. Photochem. Photobiol. B **66**, 89–106 (2002)
85. Chouikrat, R., Seve, A., Vanderesse, R., Benachour, H., Barberi-Heyob, M., Richeter, S., Raehm, L., Durand, J.O., Verelst, M., Frochot, C.: Non-polymeric nanoparticles for photodynamic therapy applications: recent developments. Curr. Med. Chem. **19**, 781–792 (2012)
86. Lu, K., He, C., Lin, W.: Nanoscale metal–organic framework for highly effective photodynamic therapy of resistant head and neck cancer. J. Am. Chem. Soc. **136**, 16712–16715 (2014)
87. Lu, K., He, C., Lin, W.: A chlorin-based nanoscale metal–organic framework for photodynamic therapy of colon cancers. J. Am. Chem. Soc. **137**, 7600–7603 (2015)
88. Carvalho, C.M.B., Brocksom, T.J., Oliveira, K.T.: Tetrabenzoporphyrins: synthetic developments and applications. Chem. Soc. Rev. **42**, 3302–3317 (2013)
89. Liu, L.H., Zhang, Y.H., Qiu, W.X., Zhang, L., Gao, F., Li, B., Xu, L., Fan, J.X., Li, Z.H., Zhang, X.Z.: Dual-stage light amplified photodynamic therapy against hypoxic tumor based on an O_2 self-sufficient nanoplatform. Small **13**, 1701621 (2017)
90. Gao, S., Zheng, P., Li, Z., Feng, X., Yan, W., Chen, S., Guo, W., Liu, D., Yang, X., Wang, S., Liang, X.J., Zhang, J.: Biomimetic O_2-evolving metal-organic framework nanoplatform for highly efficient photodynamic therapy against hypoxic tumor. Biomaterials **178**, 83–94 (2018)
91. Liu, J., Liu, T., Du, P., Zhang, L., Lei, J.: Metal–organic framework (MOF) hybrid as a tandem catalyst for enhanced therapy against hypoxic tumor cells. Angew. Chem. Int. Ed. **58**, 7808–7812 (2019)
92. Zhang, Y., Wang, F., Liu, C., Wang, Z., Kang, L., Huang, Y., Dong, K., Ren, J., Qu, X.G.: Nanozyme decorated metal–organic frameworks for enhanced photodynamic therapy. ACS Nano **12**, 651–661 (2018)
93. Zheng, D.W., Li, B., Li, C.X., Fan, J.X., Lei, Q., Li, C., Xu, Z., Zhang, X.Z.: Carbon-dot-decorated carbon nitride nanoparticles for enhanced photodynamic therapy against hypoxic tumor via water splitting. ACS Nano **10**, 8715–8722 (2016)
94. Cairns, R.A., Harris, I.S., Mak, T.W.: Regulation of cancer cell metabolism. Nat. Rev. Cancer **11**, 85–95 (2011)
95. Chen, F., Chen, J., Yang, L., Liu, J., Zhang, X., Zhang, Y., Tu, Q., Yin, D., Lin, D., Wong, P.P., Huang, D., Xing, Y., Zhao, J., Li, M., Liu, Q., Su, F., Su, S., Song, E.: Extracellular vesicle-packaged HIF-1α-stabilizing lncRNA from tumour-associated macrophages regulates aerobic glycolysis of breast cancer cells. Nat. Cell Biol. **21**, 498–510 (2019)

96. Li, S.Y., Cheng, H., Xie, B.R., Qiu, W.X., Zeng, J.Y., Li, C.X., Wan, S.S., Zhang, L., Liu, W.L., Zhang, X.Z.: Cancer cell membrane camouflaged cascade bioreactor for cancer targeted starvation and photodynamic therapy. ACS Nano **11**, 7006–7018 (2017)
97. Chen, Y.J., Mahieu, N.G., Huang, X., Singh, M., Crawford, P.A., Johnson, S.L., Gross, R.W., Schaefer, J., Patti, G.J.: Lactate metabolism is associated with mammalian mitochondria. Nat. Chem. Biol. **12**, 937–943 (2016)
98. Chen, Z.X., Liu, M.D., Zhang, M.K., Wang, S.B., Xu, L., Li, C.X., Gao, F., Xie, B.R., Zhong, Z.L., Zhang, X.Z.: Interfering with lactate-fueled respiration for enhanced photodynamic tumor therapy by a porphyrinic MOF nanoplatform. Adv. Funct. Mater. **28**, 1803498 (2018)
99. He, L., Ni, Q., Mu, J., Fan, W., Liu, L., Wang, Z., Li, L., Tang, W., Liu, Y., Cheng, Y., Tang, L., Yang, Z., Liu, Y., Zou, J., Yang, W., Jacobson, O., Zhang, F., Huang, P., Chen, X.: Solvent-assisted self-assembly of a metal–organic framework based biocatalyst for cascade reaction driven photodynamic therapy. J. Am. Chem. Soc. **142**, 6822–6832 (2020)
100. Cramer, S.L., Saha, A., Liu, J., Tadi, S., Tiziani, S., Yan, W., Triplett, K., Lamb, C., Alters, S.E., Rowlinson, S., Zhang, Y.J., Keating, M.J., Huang, P., DiGiovanni, J., Georgiou, G., Stone, E.: Systemic depletion of L-cyst(e)ine with cyst(e)inase increases reactive oxygen species and suppresses tumor growth. Nat. Med. **23**, 120–127 (2017)
101. Cheng, Q., Yu, W., Ye, J., Liu, M., Liu, W., Zhang, C., Zhang, C., Feng, J., Zhang, X.Z.: Nanotherapeutics interfere with cellular redox homeostasis for highly improved photodynamic therapy. Biomaterials **224**, 119500 (2019)
102. Zhang, W., Lu, J., Gao, X., Li, P., Zhang, W., Ma, Y., Wang, H., Tang, B.: Enhanced photodynamic therapy by reduced levels of intracellular glutathione obtained by employing a nano-MOF with Cu^{II} as the active center. Angew. Chem. Int. Ed. **57**, 4891–4896 (2018)
103. Wang, C., Cao, F., Ruan, Y., Jia, X., Zhen, W., Jiang, X.: Specific generation of singlet oxygen through the Russell mechanism in hypoxic tumors and GSH depletion by Cu-TCPP nanosheets for cancer therapy. Angew. Chem. Int. Ed. **58**, 9846–9850 (2019)
104. Miyamoto, S., Martinez, G.R., Medeiros, M.H.G., Mascio, P.: Singlet molecular oxygen generated by biological hydroperoxides. J. Photochem. Photobiol. B **139**, 24–33 (2014)
105. Melancon, M.P., Zhou, M., Li, C.: Cancer theranostics with near-infrared light-activatable multimodal nanoparticles. Acc. Chem. Res. **44**, 947–956 (2011)
106. Dykman, L., Khlebtsov, N.: Gold nanoparticles in biomedical applications: recent advances and perspectives. Chem. Soc. Rev. **41**, 2256–2282 (2012)
107. Tian, Q., Tang, M., Sun, Y., Zou, R., Chen, Z., Zhu, M., Yang, S., Wang, J., Wang, J., Hu, J.: Hydrophilic flower-like CuS superstructures as an efficient 980 nm laser-driven photothermal agent for ablation of cancer cells. Adv. Mater. **23**, 3542–3547 (2011)
108. Yang, K., Feng, L., Shi, X., Liu, Z.: Nano-graphene in biomedicine: theranostic applications. Chem. Soc. Rev. **42**, 530–547 (2013)
109. Zhu, Y.D., Chen, S.P., Zhao, H., Yang, Y., Chen, X.Q., Sun, J., Fan, H.S., Zhang, X.D.: PPy@MIL-100 nanoparticles as a pH- and near-IR-irradiation-responsive drug carrier for simultaneous photothermal therapy and chemotherapy of cancer cells. ACS Appl. Mater. Inter. **8**, 34209–34217 (2016)
110. Jiang, W., Zhang, H., Wu, J., Zhai, G., Li, Z., Luan, Y., Garg, S.: CuS@MOF-based well-designed quercetin delivery system for chemo–photothermal therapy. ACS Appl. Mater. Inter. **10**, 34513–34523 (2018)
111. Keerthiga, R., Zhao, Z., Pei, D., Fu, A.: Photodynamic nanophotosensitizers: promising materials for tumor theranostics. ACS Biomater. Sci. Eng. **6**, 5474–5485 (2020)
112. Wang, D., Wu, H., Zhou, J., Xu, P., Wang, C., Shi, R., Wang, H., Wang, H., Guo, Z., Chen, Q.: In situ one-pot synthesis of MOF–polydopamine hybrid nanogels with enhanced photothermal effect for targeted cancer therapy. Adv. Sci. **5**, 1800287 (2018)
113. Li, B., Wang, X., Chen, L., Zhou, Y., Dang, W., Chang, J., Wu, C.: Ultrathin Cu-TCPP MOF nanosheets: a new theragnostic nanoplatform with magnetic resonance/near-infrared thermal imaging for synergistic phototherapy of cancers. Theranostics **8**, 4086–4096 (2018)
114. Zhang, C., Bu, W., Ni, D., Zhang, S., Li, Q., Yao, Z., Zhang, J., Yao, H., Wang, Z., Shi, J.: Synthesis of iron nanometallic glasses and their application in cancer therapy by a localized fenton reaction. Angew. Chem. Int. Ed. **55**, 2101–2106 (2016)
115. Tang, Z., Liu, Y., He, M., Bu, W.: Chemodynamic therapy: tumour microenvironment-mediated fenton and fenton-like reactions. Angew. Chem. Int. Ed. **58**, 946–956 (2019)
116. Zhang, L., Wan, S.S., Li, C.X., Xu, L., Cheng, H., Zhang, X.Z.: An adenosine triphosphate-responsive autocatalytic fenton nanoparticle for tumor ablation with self-supplied H_2O_2 and acceleration of Fe(III)/Fe(II) conversion. Nano Lett. **18**, 7609–7618 (2018)
117. Yu, P., Li, X.D., Cheng, G.H., Zhang, X., Wu, D., Chang, J., Wang, S.: Hydrogen peroxide-generating nanomedicine for enhanced chemodynamic therapy. Chin. Chem. Lett. **32**, 2127–2138 (2021)
118. Liou, G.Y., Storz, P.: Reactive oxygen species in cancer. Free Radic. Res. **44**, 479–496 (2010)
119. Zhang, Y., Lin, L., Liu, L., Liu, F., Sheng, S., Tian, H., Chen, X.: Positive feedback nanoamplifier responded to tumor microenvironments for self-enhanced tumor imaging and therapy. Biomaterials **216**, 119255 (2019)
120. Wang, D., Zhou, J., Chen, R., Shi, R., Xia, G., Zhou, S., Liu, Z., Zhang, N., Wang, H., Guo, Z., Chen, Q.: Magnetically guided delivery of DHA and Fe ions for enhanced cancer therapy based on pH-responsive degradation of DHA-loaded Fe3O4@C@MIL-100(Fe) nanoparticles. Biomaterials **107**, 88–101 (2016)
121. Xue, T., Xu, C., Wang, Y., Wang, Y., Tian, H., Zhang, Y.: Doxorubicin-loaded nanoscale metal–organic framework for tumor-targeting combined chemotherapy and chemodynamic therapy. Biomater. Sci. **7**, 4615–4623 (2019)
122. Wang, Q., Tian, S., Ning, P.: Ferrocene-catalyzed heterogeneous fenton-like degradation of methylene blue: influence of initial solution pH. Ind. Eng. Chem. Res. **53**, 6334–6340 (2014)
123. Ornelas, C.: Application of ferrocene and its derivatives in cancer research. New J. Chem. **35**, 1973–1985 (2011)
124. Jaouen, G., Vessières, A., Top, S.: Ferrocifen type anticancer drugs. Chem. Soc. Rev. **44**, 8802–8817 (2015)
125. Fang, C., Deng, Z., Cao, G., Chu, Q., Wu, Y., Li, X., Peng, X., Han, G.: Co–ferrocene MOF/glucose oxidase as cascade nanozyme for effective tumor therapy. Adv. Funct. Mater. **30**, 1910085 (2020)
126. Ranji-Burachaloo, H., Karimi, F., Xie, K., Fu, Q., Gurr, P.A., Dunstan, D.E., Qiao, G.G.: MOF-mediated destruction of cancer using the cell's own hydrogen peroxide. ACS Appl. Mater. Inter. **9**, 33599–33608 (2017)
127. Brenner, D.J., Ward, J.F.: Constraints on energy deposition and target size of multiply damaged sites associated with DNA double-strand breaks. Int. J. Radiat. Biol. **61**, 737–748 (1992)
128. Song, G., Cheng, L., Chao, Y., Yang, K., Liu, Z.: Emerging nanotechnology and advanced materials for cancer radiation therapy. Adv. Mater. **29**, 1700996 (2017)
129. Pallares, R.M., Abergel, R.J.: Nanoparticles for targeted cancer radiotherapy. Nano Res. **13**, 2887–2897 (2020)

130. Li, S., Tan, L., Meng, X.: Nanoscale metal-organic frameworks: synthesis, biocompatibility, imaging applications, and thermal and dynamic therapy of tumors. Adv. Funct. Mater. **30**, 1908924 (2020)
131. Ma, T., Liu, Y., Wu, Q., Luo, L., Cui, Y., Wang, X., Chen, X., Tan, L., Meng, X.: Quercetin-modified metal–organic frameworks for dual sensitization of radiotherapy in tumor tissues by inhibiting the carbonic anhydrase IX. ACS Nano **13**, 4209–4219 (2019)
132. Wang, C., Volotskova, O., Lu, K., Ahmad, M., Sun, C., Xing, L., Lin, W.: Synergistic assembly of heavy metal clusters and luminescent organic bridging ligands in metal–organic frameworks for highly efficient X-ray scintillation. J. Am. Chem. Soc. **136**, 6171–6174 (2014)
133. Misawa, M., Takahashi, J.: Generation of reactive oxygen species induced by gold nanoparticles under X-ray and UV irradiations. Nanomed. Nanotechnol. **7**, 604–614 (2011)
134. Song, G., Ji, C., Liang, C., Song, X., Yi, X., Dong, Z., Yang, K., Liu, Z.: TaO_x decorated perfluorocarbon nanodroplets as oxygen reservoirs to overcome tumor hypoxia and enhance cancer radiotherapy. Biomaterials **112**, 257–263 (2017)
135. Zhu, H., Cheng, P., Chen, P., Pu, K.: Recent progress in the development of near-infrared organic photothermal and photodynamic nanotherapeutics. Biomater. Sci. **6**, 746–765 (2018)
136. Gong, H., Dong, Z., Liu, Y., Yin, S., Cheng, L., Xi, W., Xiang, J., Liu, K., Li, Y., Liu, Z.: Engineering of multifunctional nanomicelles for combined photothermal and photodynamic therapy under the guidance of multimodal imaging. Adv. Funct. Mater. **24**, 6492–6502 (2014)
137. Gai, S., Yang, G., Yang, P., He, F., Lin, J., Jin, D., Xing, B.: Recent advances in functional nanomaterials for light–triggered cancer therapy. Nano Today **19**, 146–187 (2018)
138. Wang, L., Qu, X., Zhao, Y., Weng, Y., Waterhouse, G.I.N., Yan, H., Guan, S., Zhou, S.: Exploiting single atom iron centers in a porphyrin-like MOF for efficient cancer phototherapy. ACS Appl. Mater. Interfaces **11**, 35228–35237 (2019)
139. Zhang, K., Meng, X., Cao, Y., Yang, Z., Dong, H., Zhang, Y., Lu, H., Shi, Z., Zhang, X.: Metal–organic framework nanoshuttle for synergistic photodynamic and low-temperature photothermal therapy. Adv. Funct. Mater. **28**, 1804634 (2018)
140. Liu, J., Zhang, L., Lei, J., Shen, H., Ju, H.: Multifunctional metal–organic framework nanoprobe for cathepsin B-activated cancer cell imaging and chemo-photodynamic therapy. ACS Appl. Mater. Interfaces **9**, 2150–2158 (2017)
141. Zhu, W., Yang, Y., Jin, Q., Chao, Y., Tian, L., Liu, J., Dong, Z., Liu, Z.: Two-dimensional metal-organic-framework as a unique theranostic nano-platform for nuclear imaging and chemo-photodynamic cancer therapy. Nano Res. **12**, 1307–1312 (2019)
142. Luo, Z., Jiang, L., Yang, S., Li, Z., Soh, W.M.W., Zheng, L., Loh, X.J., Wu, Y.L.: Light-induced redox-responsive smart drug delivery system by using selenium-containing polymer@MOF shell/core nanocomposite. Adv. Healthc. Mater. **8**, 1900406 (2019)
143. Feng, J., Xu, Z., Dong, P., Yu, W., Liu, F., Jiang, Q., Wang, F., Liu, X.: Stimuli-responsive multifunctional metal-organic framework nanoparticles for enhanced chemo-photothermal therapy. J. Mater. Chem. B **7**, 994–1004 (2019)
144. Zeng, J.Y., Zhang, M.K., Peng, M.Y., Gong, D., Zhang, X.Z.: Porphyrinic metal–organic frameworks coated gold nanorods as a versatile nanoplatform for combined photodynamic/photothermal/chemotherapy of tumor. Adv. Funct. Mater. **28**, 1705451 (2018)
145. Ni, K.Y., Lan, G.X., Veroneau, S.S., Duan, X.P., Song, Y., Lin, W.B.: Nanoscale metal-organic frameworks for mitochondria-targeted radiotherapy-radiodynamic therapy. Nat. Commun. **9**, 4321 (2018)
146. Cai, Z., Xin, F., Wei, Z., Wu, M., Lin, X., Du, X., Chen, G., Zhang, D., Zhang, Z., Liu, X., Yao, C.: Photodynamic therapy combined with antihypoxic signaling and CpG adjuvant as an in situ tumor vaccine based on metal–organic framework nanoparticles to boost cancer immunotherapy. Adv. Health. Mater. **9**, 1900996 (2020)
147. Shao, Y., Liu, B., Di, Z., Zhang, G., Sun, L.D., Li, L., Yan, C.H.: Engineering of upconverted metal–organic frameworks for near-infrared light-triggered combinational photodynamic/chemo-/immunotherapy against hypoxic tumors. J. Am. Chem. Soc. **142**, 3939–3946 (2020)
148. Gautam, S., Singhal, J., Lee, H.K., Chae, K.H.: Drug delivery of paracetamol by metal-organic frameworks (HKUST-1): improvised synthesis and investigations. Mater. Today Chem. **23**, 100647 (2022)
149. Wen, T., Quan, G.L., Niu, B.Y., Zhou, Y.X., Zhao, Y.T., Lu, C., Pan, X., Wu, C.N.: Versatile nanoscale metal-organic frameworks (nMOFs): an emerging 3D nanoplatform for drug delivery and therapeutic applications. Small **17**, 2005064 (2021)
150. Li, S., Tan, L., Meng, X.: Nanoscale metal - organic frameworks: synthesis, biocompatibility, imaging applications, thermal and dynamic therapy of tumors. Adv. Funct. Mater. **30**, 1908924 (2020)
151. Liu, J.T., Huang, J., Zhang, L., Lei, J.P.: Multifunctional metal-organic framework heterostructures for enhanced cancer therapy. Chem. Soc. Rev. **50**, 1188–1218 (2021)
152. Liu, W.C., Pan, Y., Zhong, Y.T., Li, B.H., Ding, Q.J., Xu, H.J., Qiu, Y.Z., Ren, F., Li, B., Muddassir, M., Liu, J.Q.: A multifunctional aminated UiO-67 metal-organic framework for enhancing antitumor cytotoxicity through bimodal drug delivery. Chem. Eng. J. **412**, 127899 (2021)
153. Liu, W.C., Yan, Q.W., Xia, C., Wang, X.X., Kumar, A., Wang, Y., Liu, Y.W., Pan, Y., Liu, J.Q.: Recent advances in cell membrane coated metal-organic frameworks (MOFs) for tumor therapy. J. Mater. Chem. B **9**, 4459–4474 (2021)
154. Sepehrpour, H., Fu, W.X., Sun, Y., Stang, P.J.: Biomedically relevant self-assembled metallacycles and metallacages. J. Am. Chem. Soc. **141**, 14005–14020 (2019)
155. Sun, Y., Chen, C.Y., Liu, J.B., Stang, P.J.: Recent developments in the construction and applications of platinum-based metallacycles and metallacages via coordination. Chem. Soc. Rev. **49**, 3889–3919 (2020)